NASA TECHNICAL NOTE

NASA TN D-3592



# USE OF REACTION WHEELS AND NONLINEAR CONTROL FOR A SATELLITE SCANNING A SMALL CELESTIAL AREA

*by Frederick G. Edwards*

*Ames Research Center*
*Moffett Field, Calif.*



NATIONAL AERONAUTICS AND SPACE ADMINISTRATION • WASHINGTON, D. C. • AUGUST 1966

# USE OF REACTION WHEELS AND NONLINEAR CONTROL FOR A SATELLITE SCANNING A SMALL CELESTIAL AREA

By Frederick G. Edwards

Ames Research Center
Moffett Field, Calif.

NATIONAL AERONAUTICS AND SPACE ADMINISTRATION

For sale by the Clearinghouse for Federal Scientific and Technical Information
Springfield, Virginia 22151 – Price $2.00

TABLE OF CONTENTS


| | Page |
|---|---|
| SUMMARY | 1 |
| INTRODUCTION | 1 |
| SYMBOLS | 2 |
| ANALYSIS | 4 |
| Vehicle Turnaround | 4 |
| General considerations | 4 |
| Position-limited command | 5 |
| Compensated position-limited command | 5 |
| Open-loop command | 6 |
| Line Scanning | 6 |
| General considerations | 6 |
| Linear controller | 7 |
| Small signal error function | 8 |
| Large signal error function | 9 |
| Time response | 11 |
| Nonlinear controller | 14 |
| Time response | 16 |
| Torque decay problems | 16 |
| Switching curve approach | 18 |
| Time constant approach | 18 |
| Dual-mode controller | 19 |
| ANALOG COMPUTER SIMULATION | 21 |
| RESULTS AND DISCUSSION | 22 |
| Scan System Error Response | 23 |
| Turnaround Performance | 25 |
| Complete Systems | 26 |
| SUMMARY OF RESULTS | 27 |
| APPENDIX A | 29 |
| REFERENCES | 31 |
| TABLE I | 32 |
| TABLE II | 32 |
| FIGURES | 33 |

# USE OF REACTION WHEELS AND NONLINEAR CONTROL FOR A SATELLITE SCANNING A SMALL CELESTIAL AREA

By Frederick G. Edwards
Ames Research Center

## SUMMARY

Several schemes have been studied for controlling the raster scanning maneuver of a satellite system scanning a small celestial area. The control torque is supplied by an inertia wheel in combination with a torque motor. The entire satellite maneuvers in two phases, a scanning phase and a turn-around phase at the end of each scan line. The study of the scanning phase considers a single control loop with various modifications to the controller component of the loop. Controllers of the linear, nonlinear, and dual-mode types are considered. The scanning system was analyzed on the basis of response to large disturbances, tracking accuracy, and performance degradation due to the buildup of inertia wheel momentum. A theoretical investigation, consisting of a linear analysis, a nonlinear analysis based on a phase plane approach, and an analog computer study, indicates that the system with either the linear or dual-mode controller can perform the high precision scan required. The nonlinear controllers were unacceptable because of their undesirable "jitter" characteristics.

Vehicle turnaround performance was found to be very sensitive to the geometry of the command input signal. Various shape signals were analyzed. A complex adaptive type of command signal which adjusts to changes in control torque level was found to be necessary for effecting the smooth, efficient turnaround desired.

The effect of inertia wheel saturation was found to be pronounced during scan and turnaround. When operating with high wheel speeds, the system can be subject to large overshoots and chattering. Various procedures are presented to compensate for this loss in performance. In all cases, the torque motor must be operated over a restricted speed range.

## INTRODUCTION

For a vehicle, such as the Advanced Orbiting Solar Observatory, the demands on the control system to achieve high pointing accuracies are quite stringent. The raster scanning mode presents some of the more demanding requirements of the attitude control system. The criteria for the performance of the raster scanning mode are discussed in detail in reference 1. The system is required to scan an area, centered on the solar disk or on a prescribed point in the vicinity of the sun, within a specified accuracy. An artist's conception of the spacecraft's raster scanning operation is shown in figure 1.

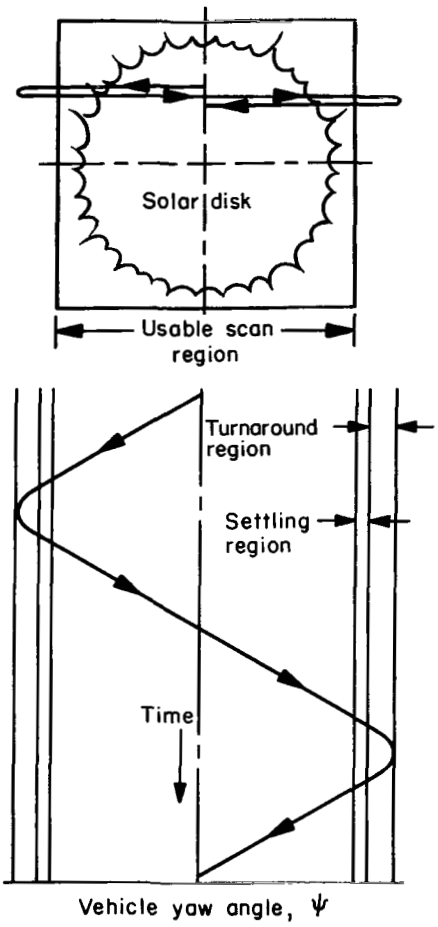


Sketch (a)

Sketch (a) shows more details of the vehicle motions. The entire vehicle is maneuvered about the yaw axis and small pitching motions are introduced as the scan reverses at the end of each line. This analysis will be concerned only with the dominant motions about the yaw axis and will therefore be restricted to a single-axis control system. An inertia wheel in combination with a torque-motor will be considered as a control torque source. The use of inertia wheels for controlling the attitude of satellite vehicles is discussed in reference 2.

The problem will be to devise a system to control the raster scan maneuver and satisfy the criteria of high pointing accuracy, smooth and efficient turnaround, and adequate response to internal torque disturbances. The maneuver has two phases of operation: (1) scanning a line and (2) turning around. They are examined separately.

The analysis of the turnaround is brief. After a method of attack is discussed, a few possible schemes are examined and their performance compared. The studies of scan control are detailed. Several controllers are analyzed to determine which control will satisfy the performance requirements of the advanced OSO. The two phases are then combined in an analog computer study of the complete raster scan maneuver. The relative performance of the various systems based on specified problem criteria are presented.

Disturbance torques on the vehicle are of two types: external and internal. The external disturbances, which are due to solar pressures, gravity gradient, magnetic field, and atmospheric drag, have long period variations and are relatively small. The peak values of each have been estimated to be less than $7 \times 10^3$ dyne-cm. These torques will be neglected. An internal torque disturbance resulting from motions of machinery within the spacecraft is relatively large and is considered in this study.

## SYMBOLS

$I_z$ moment of inertia of satellite vehicle, gm-cm$^2$

$J_m$ moment of inertia of inertia wheel, gm-cm$^2$

$K_l$ loop gain, V/arc min

$K_m$ torque motor back emf gain, radians/sec/V

$K_r$ gain of differentiating network, V/arc min/sec

$K_t$ torque motor gain, dyne-cm/V

$K_\epsilon$ motor amplifier gain, V/V

P maximum value of first-order rate term in dual-mode switching equation

S transform variable, $sec^{-1}$

Sat saturation

Sign algebraic sign of quantity

T control torque, dyne-cm

$T_d$ internal disturbance torque, dyne-cm

$T_{min}$ minimum torque level of system, dyne-cm

$T_s$ stall torque, dyne-cm

t time, sec

$t_s$ total settling time for a given initial condition, sec

V voltage input to motor, V

$W_w$ angular velocity of inertia wheel, radians/sec

$\alpha$ $\frac{T}{I_z} - \frac{\dot{\psi}_e}{\tau_m}$, arc min/$sec^2$

$\Delta$ incremental change

$\Delta t$ time increment, sec

$\epsilon$ error signal, V

$\zeta$ normalized damping ratio

$\tau_m$ time constant of torque motor and inertia wheel, sec

$\tau_r$ time constant of differentiator network, sec

$\tau_s$ time constant of sun sensor, sec

$\tau_t$ time constant of tachometer, sec

$\psi$ angular position of satellite vehicle, arc min

| | |
|---|---|
| $\dot{\psi}$ | angular rate of satellite vehicle, arc min/sec |
| $\omega_n$ | system natural frequency, radians/sec |

Subscripts

| | |
|---|---|
| o | initial value of variable |
| 1,2,3,... | intermediate values of variable |
| c | commanded value |
| e | error |
| max | maximum allowable value of quantity |
| min | minimum allowable value of quantity |
| ss | steady state |
| t | total |

## ANALYSIS

In this section several possible control schemes will be presented for performing the raster scan maneuver. Motions will be considered about a single axis of freedom. The turnaround phase and the line scanning phase of the maneuver will be analyzed separately. Five possible schemes for generating the turnaround command signal will be explored, starting with a simplified closed-loop system and progressing to more complex adaptive and open-loop type systems. The line scanning phase of the study will consider a single control loop with various modifications to the controller component of the loop. Five different controllers are analyzed, one linear switch curve type, three nonlinear switch curve types, and one dual-mode type. The turnaround phase of this study will be considered first.

### Vehicle Turnaround

General considerations.- The problem is how to turn the whole vehicle most expeditiously from one scan line to the next. To accomplish this, the maximum available control torque is applied at the end of a line of scan in the direction to oppose the vehicle motion. The torque is applied until the vehicle is traveling in the opposite direction at the correct velocity. A smooth reversal in vehicle scan direction is desired. The turnaround maneuver and its related settling, or damping sequence, takes place outside a usable scan region. When the vehicle again enters the scan area, the position and velocity error should be small so that the transition into the line scanning phase is smooth. In this maneuver as little time as possible should be expended.

Sketch (a) indicates that a sawtooth shaped command signal would be effective in producing the desired motions of the spacecraft, but it will be shown that a simple sawtooth command signal is not efficient for controlling the vehicle through the turnaround phase. As indicated in sketch (b) half the available time for the turnaround maneuver is not used since the control system senses no error signal until the scan command has reached the extreme of the saw tooth. The command signal may be modified so that a greater portion of the turnaround time is used. Three approaches were studied.

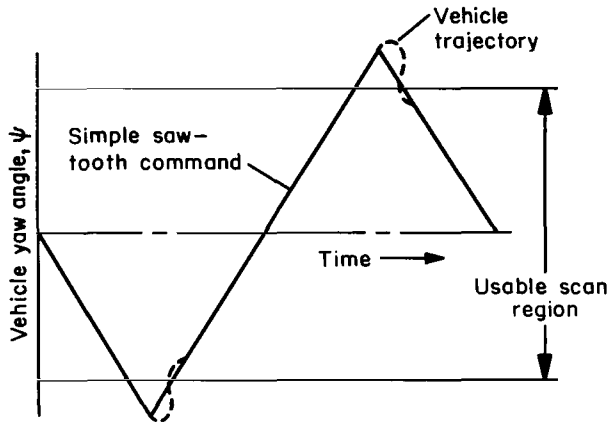


Sketch (b)

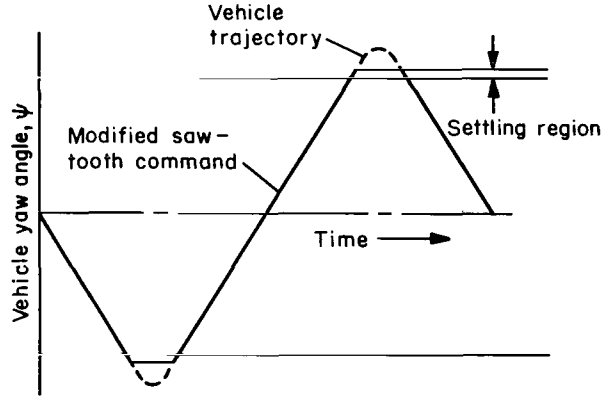


Sketch (c)

Position-limited command.- Sketch (c) shows the shape of the position command input signal. The flattened apex of this signal will cause a saturation level signal to the control torque motor and thus result in maximum available torque to turn the vehicle. The duration of the saturation may be selected to correspond to the turnaround time for the stall or mean torque level. Consequently, the performance of this system may be expected to be degraded at other than this mean level.

One other problem may be anticipated with this type command input. Just prior to completion of the turnaround maneuver when the position error is relatively small, the control system would attempt to aline the vehicle trajectory to the effective zero rate command input, causing an undesirable reversal of the torque signal. When the command is again a ramp, the system would immediately switch to the correct sign, but this "undesirable switch" would introduce an undesirable error into the system. The extent to which these problems degrade the performance will be discussed in detail in a later section.

Compensated position-limited command.- The position-limited command may be modified to improve performance for operating at other than the stall torque level. The extent of the command signal flattening may be made variable and a function of the control torque level of the system. This is accomplished by measuring the inertia wheel speed, relating this to the available control torque, and then determining the duration of the flattening required for the turnaround maneuver. In essence, the command geometry is matched to the

expected vehicle trajectory as indicated in sketch (d). In this sense, the command circuit may be thought of as an adaptive system. The obvious advantage of this system is that it eliminates overshoots and undershoots that would appear in the simple position-limited system, but it also permits biasing the limiter so as to eliminate the undesirable switching mentioned in the previous section.

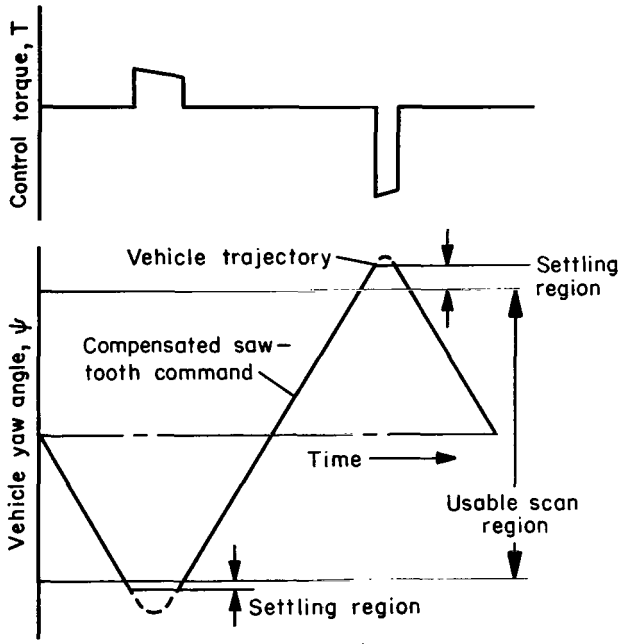


Sketch (d)

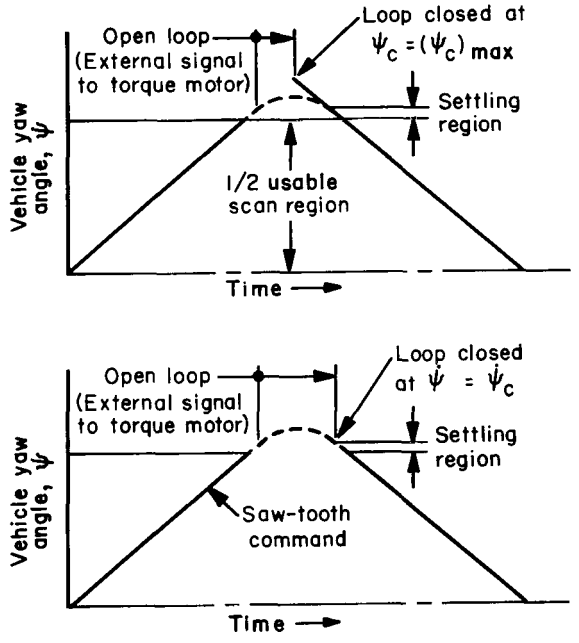


Sketch (e)

Open-loop command.- An external control signal also might be used for the turnaround. The logic for opening and closing the loop could be quite simple. The feedback loop would be opened by the position command signal outside the useful scan zone. An external constant-level signal would energize the torque motor to produce the maximum available torque during the turnaround. At the completion of the maneuver the loop would be closed. The time of loop closing may be controlled by the vehicle position command (position sensitive closing) or by the vehicle rate error (rate sensitive closing). The shape of the command signals for these two approaches is shown in sketch (e). There is a discontinuity in the position command signal for the open-loop portions when the external signal commands the vehicle. For position sensitive closing (upper figure) the loop is closed at the apex of the saw tooth which is known even during the open-loop portion. In the case of rate sensitive closing (lower figure) the loop is closed when the vehicle rate equals the commanded rate. The performance with each type of control will be demonstrated in the later section on analog computer simulation.

## Line Scanning

General considerations.- The scan problem can be stated as follows. Starting with an initial pointing error resulting from the turnaround, get the vehicle into the proper position with the correct steady velocity as soon as

possible. Perform the steady scan within a prescribed amount of jitter and within a specified position error. Different type controllers will be considered in analyzing the system for conducting this scan.

A block diagram for the single-axis control scheme is shown in figure 2. The vehicle scan position is measured by the sun sensor and compared with the commanded position. The difference is used as the error signal for vehicle control. The error signal is processed by the controller to produce the control signal for transition from the initial to the commanded state. The controller is capable of providing linear or nonlinear relationships between the input and output signal. The torque motor is assumed to have a linear torque-speed relationship. The transfer function for the motor-inertia wheel combination, derived in appendix A, is of the form

$$T(S) = k_t\left(V_{in} - \frac{W_{w_o}}{K_m S}\right)\frac{\tau_m S}{\tau_m S + 1} \tag{1}$$

where the form of the input voltage $V_{in}$ will be specified in accordance with the type of controller used in the control-system loop. The stored momentum of the inertia wheel is proportional to the initial wheel speed, which is designated $W_{w_o}$ in equation (1).

The satellite body in this single-axis study is represented by the function $1/I_z S^2$ in figure 2.

To simplify the following analysis the dynamics of the sun sensor are neglected. This assumption is valid since the basic design criteria for such a sensor would require that the response be fast compared to the attitude control system. The design criteria for the sun sensor are discussed in reference 3.

Linear controller.- The linear switch curve controller shown in sketch (f) uses the transfer function for the controller network

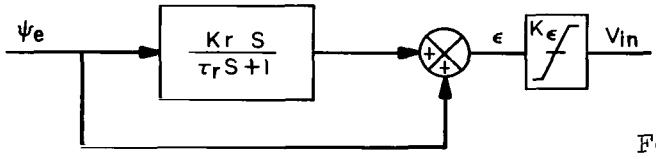


Sketch (f)

$$\frac{\epsilon}{\psi_e} = \frac{(K_r + \tau_r)S + 1}{\tau_r S + 1} \tag{2}$$

For a theoretical analysis it will be convenient to consider an approximation for this controller function. The resulting transfer function for the control system will then be limited to second order to allow a phase plane representation of the motion. The validity of the approximation requires some discussion.

Expanding the denominator of equation (2) in a series gives:

$$\frac{\epsilon}{\psi_e} = [(K_r + \tau_r)S + 1][1 - \tau_r S + \ldots (-1)^n(\tau_r S)^n] \tag{3}$$

$$\frac{\epsilon}{\psi_e} = 1 + K_r S - \tau_r K_r S^2 + \ldots \tag{4}$$

The time constant $\tau_r$ associated with the lag is designed to be small in comparison to $K_r$ ($\tau_r < 0.1K_r$). Thus it becomes evident that the coefficients of the second and higher order term are negligible in comparison with the first. A reasonable approximation for the controller network thus would be:

$$\frac{\epsilon}{\psi_e} = 1 + K_r S \tag{5}$$

The switching function in the time domain will be

$$\epsilon = \psi_e + K_r \dot{\psi}_e \tag{6}$$

The output $\epsilon$ is fed to a limiter which obeys the following equations:

$$\text{for} \quad |K_\epsilon \epsilon| \leq V_{max} \quad \text{then} \quad V_{in} = K_\epsilon \epsilon \tag{7}$$

$$\text{for} \quad |K_\epsilon \epsilon| > V_{max} \quad \text{then} \quad V_{in} = V_{max} \ \text{Sgn} \ K_\epsilon \epsilon \tag{8}$$

Small signal error functions: If the above simplification of the controller network is made, the closed-loop transfer function for the control system may be obtained with a second-order characteristic equation. The relationship of the vehicle position error and the commands, torque disturbance, and initial wheel speed may be obtained in the form

$$\psi_e(S) = \frac{\left(S\psi_c + \frac{T_d}{I_z S}\right)\left(S + \frac{1}{\tau_m}\right) + \frac{J_m W_{w_o}}{\tau_m I_z S}}{S^2 + \left(\frac{1}{\tau_m} + K_r \omega_n^2\right) S + \omega_n^2} \tag{9}$$

where the system frequency is

$$\omega_n^2 = \frac{K_l}{\tau_m} \tag{10}$$

the loop gain

$$K_l = \frac{K_\epsilon K_m J_m}{I_z} \tag{11}$$

Also, from this expression the damping coefficient is seen to be

$$\xi = \frac{1}{2\tau_m \omega_n} + \frac{K_r \omega_n}{2} \tag{12}$$

The steady-state error resulting from a step input, a ramp command, a torque impulse, and an initial wheel speed may be determined by applying the final-value theorem to the error equation. This has been done and the results are stated here.

Step position command

$$\frac{\psi_{e_{ss}}}{\psi_c} = 0 \tag{13}$$

Ramp command

$$\frac{\psi_{e_{ss}}}{\dot{\psi}_c} = \frac{1}{\tau_m \omega_n^2} \tag{14}$$

Torque pulse disturbance

$$\frac{\psi_{e_{ss}}}{T_d} = \frac{\Delta t}{I_z \tau_m \omega_n^2} \tag{15}$$

Inertia wheel speed

$$\frac{\psi_{e_{ss}}}{W_{w_o}} = \frac{J_m}{I_z \tau_m \omega_n^2} \tag{16}$$

These steady-state results will be used in the analog computer section of this paper to specify the gains for a practical scan system.

The related time equation of the system for operation within the proportional zone is determined by taking the inverse Laplace transform of equation (9). If the initial conditions of $\psi_{e_o}$ and $\dot{\psi}_{e_o}$ are specified, the position error equation may be determined as a function of $\omega_n$ and $\xi$.

$$\psi_e(t) = A_o \frac{\xi e^{-\xi\omega_n t}}{\sqrt{1 - \xi^2}} \sin(\omega_n \sqrt{1 - \xi^2}\, t + \beta_o) \tag{17}$$

where

$$A_o^2 = \left(\psi_{e_o} + \frac{\dot{\psi}_{e_o}}{\xi\omega_n}\right)^2 + \left(\psi_{e_o} \frac{\sqrt{1 - \xi^2}}{\xi}\right)^2 \tag{18}$$

and

$$\beta_o = \tan^{-1} \frac{\psi_{e_o} \sqrt{1 - \xi^2}/\xi}{\psi_{e_o} + \dot{\psi}_{e_o}/\xi\omega_n} \tag{19}$$

The corresponding rate equation is found by differentiating $\psi_e(t)$ with respect to time. This results in

$$\dot{\psi}_e(t) = A_o \omega_n e^{-\xi\omega_n t}\left[\cos(\omega_n \sqrt{1 - \xi^2}\, t + \beta_o) - \frac{\xi}{\sqrt{1 - \xi^2}} \sin(\omega_n \sqrt{1 - \xi^2}\, t + \beta_o)\right] \tag{20}$$

Equations (17) and (20) will prove useful for evaluating response times for the system with the linear controller during operation within the proportional region.

Large signal error function: For large errors in the vehicle position and rate, the system will be operating outside the range of proportional control.

In this region a different set of trajectory equations will define the vehicle motions. The bounds of the region are defined by equation (7). In terms of the state variables for this linear switch curve system, the boundary equation will be:

$$\left|K_e(\psi_e + K_r\dot{\psi}_e)\right| = V_{max} \tag{21}$$

We will now proceed to determine the shape of the vehicle trajectories outside this region of proportional control. The dynamical equation of the vehicle motion is of the general form

$$\ddot{\psi}(t) = \frac{T(t)}{I_z} \tag{22}$$

where the torque $T(t)$ may be expressed in terms of the input voltage, $V_{in}$ and and the wheel speed $W_w$, by performing the inverse Laplace transform of equation (A2). This gives the expression

$$\ddot{\psi}(t) = \frac{K_t}{I_z}\left[V_{in} - \frac{W_w(t)}{K_m}\right] \tag{23}$$

If the external torque disturbances are zero, the conservation of angular momentum requires that

$$[W_w(t) - W_{w_o}]J_m = [\dot{\psi}(t) - \dot{\psi}_o]I_z \tag{24}$$

The solution of this equation for the wheel speed $W_w(t)$ is substituted into equation (23) to obtain the expression

$$\ddot{\psi}(t) = \frac{K_T}{I_z}\left(V_{in} - \frac{1}{K_m}\left\{W_{w_o} + \frac{I}{J_m}[\dot{\psi}(t) - \dot{\psi}_o]\right\}\right) \tag{25}$$

or simply

$$\ddot{\psi}(t) = \frac{T_o}{I_z} - \frac{1}{\tau_m}[\dot{\psi}(t) - \dot{\psi}_o] \tag{26}$$

In equation (26) $K_T(V_{in} - W_{wo}/K_m)$ is replaced by its equivalent expression $T_o$, where $T_o$ is the magnitude of the initial torque at time equal to zero. (This equivalence may be verified for a step voltage input from equation (1) by use of the initial value theorem.)

Equation (26) may now be written in terms of the error, where $\psi_e$ is defined as $\psi_e \equiv \psi_c - \psi$. If the command input, $\psi_c$, is limited to a combination of a step and ramp, the following expression is determined for the system differential equation.

$$\ddot{\psi}_e(t) = -\frac{T_o}{I_z} + \frac{1}{\tau_m}[\dot{\psi}_{e_o} - \dot{\psi}_e(t)] \tag{27}$$

Expressing $\ddot{\psi}_e(t)$ as $\frac{d\dot{\psi}_e}{d\psi_e} \cdot \frac{d\psi_e}{dt}$ and rearranging terms, we put equation (27)

in a form convenient to integrate

$$d\psi_e = \frac{-\tau_m \dot{\psi}_e \, d\dot{\psi}_e}{\dot{\psi}_e + \tau_m\left(\frac{T_o}{I_z} - \frac{\dot{\psi}_{e_o}}{\tau_m}\right)} \tag{28}$$

Integrating, we obtain the relationship of position and rate error,

$$\psi_e = -\tau_m\dot{\psi}_e + \tau_m^2\left(\frac{T_o}{I_z} - \frac{\dot{\psi}_{e_o}}{\tau_m}\right)\ln\left[\dot{\psi}_e + \tau_m\left(\frac{T_o}{I_z} - \frac{\dot{\psi}_{e_o}}{\tau_m}\right)\right] + C \tag{29}$$

Equation (29) represents the general trajectories of the motion in the phase plane ($\psi_e$ vs $\dot{\psi}_e$). The constant of integration $C$ is determined by specifying the initial position and rate errors, $\psi_{e_o}$ and $\dot{\psi}_{e_o}$; equation (29) then becomes

$$\psi_e = -\tau_m(\dot{\psi}_e - \dot{\psi}_{e_o}) + \tau_m^2\alpha_o \ln\left(\frac{\dot{\psi}_e + \tau_m\alpha_o}{\dot{\psi}_{e_o} + \tau_m\alpha_o}\right) + \psi_e \tag{30}$$

where $\alpha_o$ is defined as

$$\alpha_o \equiv \frac{T_o}{I_z} - \frac{\dot{\psi}_{e_o}}{\tau_m} \tag{31}$$

Time response: A typical phase-plane trajectory representing the vehicle motion will be both within the proportional region and in the saturated region. For large initial errors the trajectory will be composed of several distinct segments. The computation of the response time will be carried out on a piecewise basis. As an example, the phase-plane trajectory in sketch (g) is divided into four segments, two in the saturated region and two in the proportional region. The boundaries of the proportional control region of sketch (g) are phase-plane plots of equation (21) for positive and negative values of $V_{max}$. The four segments are representative of the different types of segments which would be generally encountered. The time increment for each segment is determined separately. The total settling time will be obtained by summing the time increments required to traverse the individual trajectory segments.

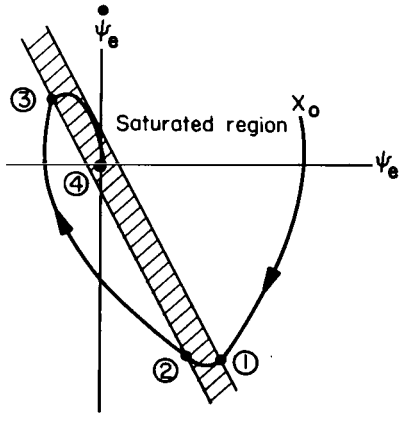

Sketch (g)

$$t_s = \sum_{o}^{n} \Delta t_n \tag{32}$$

The transient time, for a particular set of initial conditions for which the trajectory remains within the proportional zone, is determined by using only the exponential envelope of the curve expressed in equation (17). A

typical trajectory of this type is shown in sketch (h). The time for the envelope of the error function to decay to a value smaller than the allowable tracking error will be designated the transient time. From equation (17), this is obtained in the form:

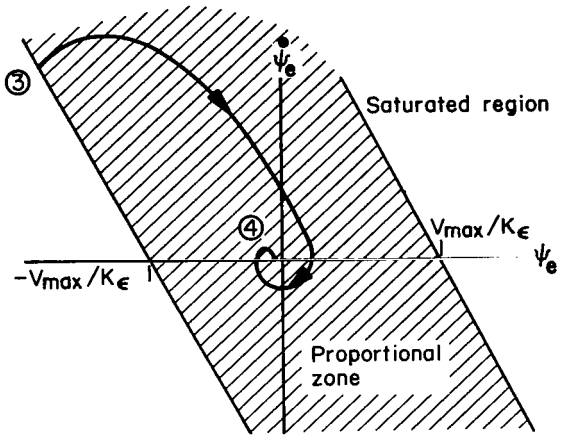

Sketch (h)

$$\Delta t_{3-4} = \frac{1}{\xi\omega_n} \ln \frac{A_o}{\psi_{e_{ss}} \frac{\sqrt{1-\xi^2}}{\xi}} \tag{33}$$

when $\psi_{e_{ss}}$ is the allowable steady-state tracking error (ramp input) and $A_o$ defines the initial conditions of error and error rate (eq. (18)).

The situation in which the trajectory passes through the proportional zone and into the saturated region must be handled differently. This is the type of trajectory shown between points 1 and 2 in sketch (g). If the error rate changes appreciably during the transition, an accurate expression may be obtained by evaluating the expression

$$\Delta t_{1-2} = \int_{\psi_{e_1}}^{\psi_{e_2}} \frac{d\psi_e}{\dot{\psi}_e} \tag{34}$$

If the error rate does not change appreciably, then a good approximation of time may be obtained by assuming a constant rate error. During the time interval, this results in a much simpler expression of the form

$$\Delta t_{1-2} = \frac{\Delta\psi_e}{\dot{\psi}_{e_1}} \tag{35}$$

where $\Delta\psi_e$ is the change in the value of $\psi_e$ which will be the width of the proportional zone. This width is determined by evaluating the change in $\psi_e$ across the boundaries for constant rate error from equation (21)

$$\Delta\psi_e = \Delta\left(\frac{V_{max}}{K_\epsilon}\right), \qquad \text{since} \qquad \Delta\dot{\psi}_e = 0 \tag{36}$$

$$\Delta\psi_e = \frac{2V_{max}}{K_\epsilon} \tag{37}$$

thus the time increment will be

$$\Delta t_{1-2} = \frac{2V_{max}/K_\epsilon}{\dot{\psi}_{e_1}} \tag{38}$$

If the initial error is large in comparison to the width of the proportional zone, then the trajectory would pass through this zone rapidly. The time increment involved may represent a small addition to the total transient time involved. A reasonable approximation could then be obtained by neglecting the small signal segments as indicated in sketch (i). This type of approach is described fully in reference 4 and is known as the switching time method.

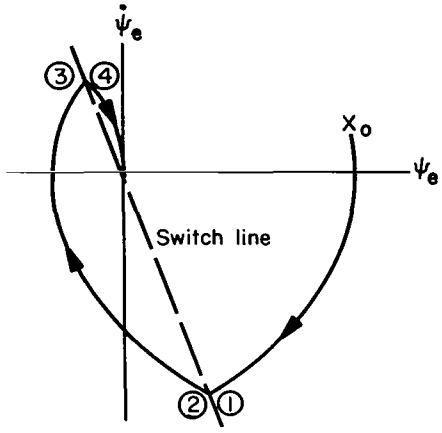

Sketch (i)

The expressions for the transient times in the proportional regions have been found and are represented by equations (32) and (38). The time required to reverse a trajectory segment in the saturated region will now be developed from equation (28). The time increment is defined as in equation (33)

$$\Delta t_{o-1} = \int_{\psi_{e_o}}^{\psi_{e_1}} \frac{d\psi_e}{\dot{\psi}_e} \tag{39}$$

where the subscripts refer to the trajectory segment from 0 to 1 in sketch (g). Substituting equation (28) into (39), integrating and substituting the appropriate limits, we obtain the incremental time

$$\Delta t_{o-1} = -\tau_m \ln\left(\frac{\dot{\psi}_{e_1} + \tau_m\alpha_o}{\dot{\psi}_{e_o} + \tau_m\alpha_o}\right) \tag{40}$$

The error rate $\dot{\psi}_{e_1}$ at which the trajectory enters the proportional zone is determined from the simultaneous solution of the boundary equation (21) and the trajectory equation (30). This resulting equation may be expanded in a Maclaurin series to give the approximate result:

$$\dot{\psi}_{e_1} = \alpha_o K_r - \left\{(\alpha_o K_r)^2 + \left[\dot{\psi}_{e_o}^2 + 2\alpha_o\left(\psi_{e_o} - \frac{V_{max}}{K_\epsilon}\right)\right]\right\}^{1/2} \tag{41}$$

where $\alpha_o$ is defined in equation (31).

The corresponding position error $\psi_{e_1}$ is:

$$\psi_{e_1} = \frac{V_{max}}{K_\epsilon} - K_r\dot{\psi}_{e_1} \tag{42}$$

The torque magnitude at the time, $t = t_1$ is:

$$T_1 = T_o - \frac{I_z(\dot{\psi}_{e_o} - \dot{\psi}_{e_1})}{\tau_m} \tag{43}$$

The trajectory segment from 2 to 3 in sketch (g) may be handled in the same manner, the difference being that the control torque for this portion is negative; whereas for the initial segment, it was positive. The increment of time for this portion may be expressed as:

$$\Delta t_{2\text{-}3} = -\tau_m \ln \frac{\dot{\psi}_{e_3} + \tau_m \alpha_2}{\dot{\psi}_{e_2} + \tau_m \alpha_2} \tag{44}$$

where

$$\alpha_2 \equiv \frac{T_2}{I_z} - \frac{\dot{\psi}_{e_2}}{\tau_m}$$

with

$$T_2 = -T_o - \frac{I_z(\dot{\psi}_{e_o} - \dot{\psi}_{e_2})}{\tau_m}$$

As noted previously, $\dot{\psi}_{e_2} \approx \dot{\psi}_{e_1}$.

The error rate $\dot{\psi}_{e_3}$ is determined as was equation (41) by the simultaneous solution of the trajectory and the boundary. This result will be

$$\dot{\psi}_{e_3} = \alpha_2 K_r + \left\{ (\alpha_2 K_r)^2 + \left[ \dot{\psi}_{e_2}^2 + 2\alpha_2 \left( \psi_{e_2} - \frac{V_{max}}{K_\epsilon} \right) \right] \right\}^{1/2} \tag{45}$$

Nonlinear controller.- It is noted that in the previous section the trajectories for the system incorporating the linear controller with linear switching lines will overshoot the origin for all but small initial error conditions (see sketch (g)). This characteristic will result in long transient times for the system. The overshooting may be eliminated if the switching function is modified so that the torque reversal occurs at the times corresponding to the minimum time response for all initial error conditions. Systems of this type are discussed in references 5, 6, and 7. For minimum time response, the system will operate at the maximum available control torque at all times. The operation of the system may be explained with the aid of a phase-plane plot such as presented in sketch (j). The trajectory appearing in the sketch is a typical one which relates the motions of the vehicle, its position, and rate error for a constant voltage input. The two branches which pass through the origin are the terminal trajectories for every arbitrary set of initial conditions. These trajectories are used as the switching curves (ref. 5). The switching network performs as follows: For an initial set of error conditions the controller network determines the proper sign for the torque motor input voltage. The torque motor will accelerate the vehicle along an appropriate trajectory until it

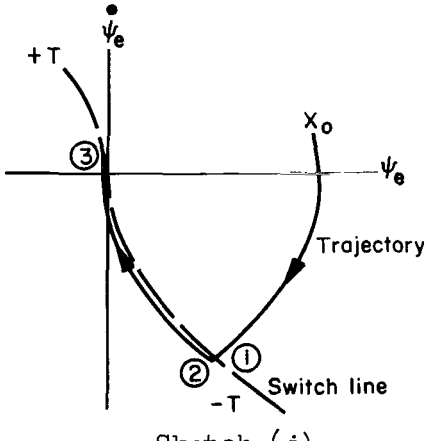

Sketch (j)

intersects the switching curve. At the switch line the torque signal is reversed, the vehicle will follow this trajectory into the origin and settle the error with only one sign reversal.

The equation for these switching curves is determined from equation (29) for the general trajectory of the motion in the saturated region of the phase plane.

Since the switching lines are represented by the two trajectories which pass through the origin, then the constant C in equation (29) is evaluated by substituting the terminal condition of $\psi_e = 0$ and $\dot{\psi}_e = 0$ to obtain

$$C = -\tau_m^2 \alpha_o \ln \tau_m \alpha_o \tag{46}$$

The switching lines are then

$$\psi_e = -\tau_m \dot{\psi}_e + \tau_m^2 \alpha_o \ln\left(1 + \frac{\dot{\psi}_e}{\tau_m \alpha_o}\right) \tag{47}$$

From this equation the control function is

$$\epsilon = \psi_e + \tau_m \dot{\psi}_e - \tau_m^2 \alpha_o \ln\left(1 + \frac{\dot{\psi}_e}{\tau_m \alpha_o}\right) \tag{48}$$

The controller network is required to solve equation (48). The direction of the control torque will change when $\epsilon$ changes sign. This means that the system operates at either full positive or full negative control torque even for small error magnitudes. The controllers which produce this type of output will will be referred to under the general name of nonlinear controllers. This bang-bang output is also typical of relay systems discussed in references 6 and 7. It is indicated in these references that small time lags and hysteresis in the system will cause the motion to terminate in a limit cycle operating near the origin.

A computer mechanization of equation (48) is complex in this form due to the presence of the logarithmic term. The expression is simplified by expanding the log term in a Maclaurin series for log (1 + x)

$$\epsilon = \psi_e + \frac{\dot{\psi}_e^2}{2\alpha_o} - \frac{\dot{\psi}_e^3}{3\tau_m \alpha_o^2} + \cdots \tag{49}$$

If the torque motor time constant is large, then a good approximation for the switching function may be obtained in the form

$$\epsilon = \psi_e + \frac{\dot{\psi}_e |\dot{\psi}_e|}{2T_s/I_z} \tag{50}$$

Solutions to equation (50) for $\epsilon = 0$ give the approximations of the two terminal trajectories shown in sketch (k). The term $\dot{\psi}_e|\dot{\psi}_e|$ is the sign square of the yaw rate error and, in effect, is used to eliminate that half of the trajectories (switch lines) which lead away from the origin. These parts have no real meaning for this controlled system. The neglected parts are the dashed lines leading away from the origin and located in the first and third quadrants of sketch (k). The controller network is shown in sketch (l).

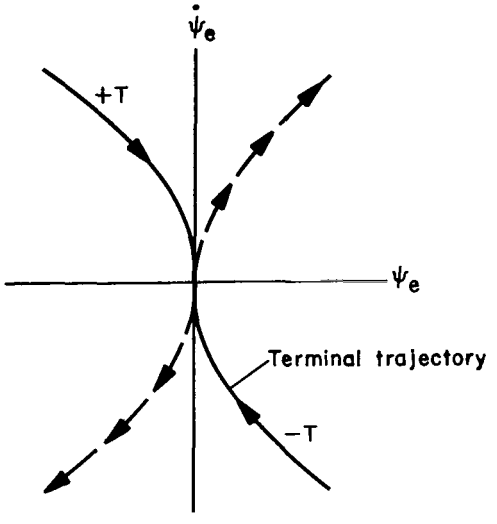


Sketch (k)

Time response: For the system with this nonlinear controller there will be only two trajectory segments as indicated in sketch (j). The total settling time will be the sum of these two time increments. Since the torque motor time constant is assumed to be large, equation (40) for time response in the saturated region will reduce to

$$\Delta t_{0-1} = \frac{\dot{\psi}_{e_0} - \dot{\psi}_{e_1}}{T_s/I_z} \tag{51}$$

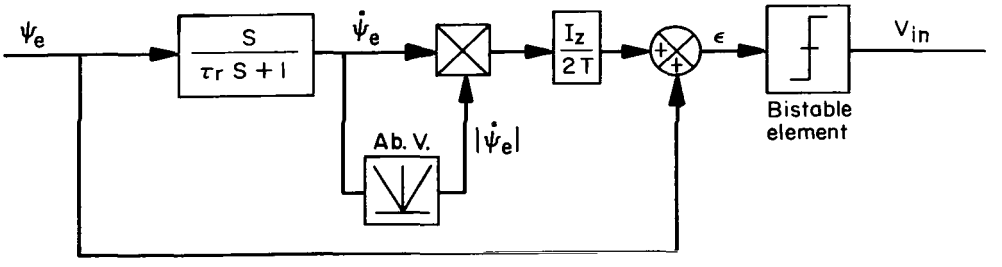


Sketch (l)

where $T_s$ is the stall torque. The time increment for the segment from 1 to 2 may be found to be

$$\Delta t_{1-2} = \frac{-\dot{\psi}_{e_1}}{T_s/I_z} \tag{52}$$

The total settling time expressed in terms of initial conditions of $\psi_{e_0}$ and $\dot{\psi}_{e_0}$ results in the equation:

$$t_s = \left[\frac{4\psi_{e_0}}{T_s/I_z} + \frac{2\dot{\psi}_{e_0}^2}{(T_s/I_z)^2}\right]^{1/2} + \frac{\dot{\psi}_{e_0}}{T_s/I_z} \tag{53}$$

Torque decay problems.- In the previous section the switching function, equation (50), represents minimum time switching only for situations in which the motor time constant is equal to infinity and the control torque magnitude is essentially constant and equal to the stall torque at all times during the error correcting maneuver. For the operation of a practical system the motor time constant is much less than infinity and the initial torque level may vary

over a wide range, depending on the momentum which has been stored in the inertia wheel. The effects of this variation in control torque level will be discussed next.

It was stated previously that the initial torque level may be expressed as

$$T_o = K_t\left(V_{in} - \frac{W_{w_o}}{K_m}\right)$$

or in more fundamental terms

$$T_o = T_s - \frac{J_m}{\tau_m} W_{w_o} \tag{54}$$

where $T_s$ is the stall torque (rating of the motor at $W_w = 0$) and $J_m W_{w_o}$ is the initial momentum of the wheel. This relation expresses the fact that the available control torque decays as a function of wheel speed at a rate $-(J_m/\tau_m)$. A typical torque-speed curve for such a motor could be represented by sketch (m). As an example of the type of problems which would be encountered with such a motor, consider its operation in a system incorporating the nonlinear controller presented in the previous section. If an error correction maneuver is performed with a negative momentum stored by the inertia wheel the system would be performing in the region indicated by the arrows in sketch (m). A higher torque level is applied during the acceleration (+T) than during the deceleration (-T) periods. This change in torque level will result in reshaped trajectories in the phase plane. For the system operating in the range of wheel speeds indicated above, the phase-plane plot would appear as in sketch (n). The steep initial trajectory from 0 to 1 corresponds to the high level torque from 0 to 1 in sketch (m). The shallow segment indicates a lower torque level from 2 to 3. This trajectory will overshoot the origin. If the trajectory segments are traced for the condition of positive wheel speed, the terminal trajectory will tend to undershoot the origin, which is equally objectionable and will result in a condition known as chattering. The trajectory will alternately be driven back and forth across the switching line while proceeding toward the origin. Motions of this type are

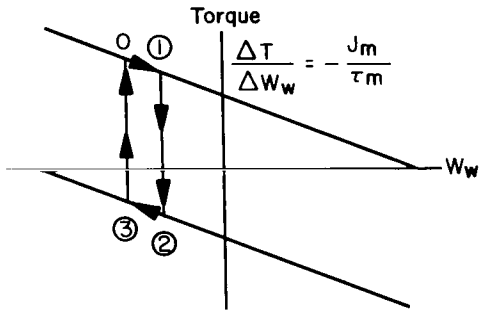


Sketch (m)

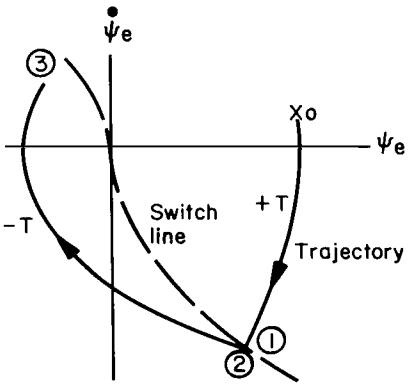


Sketch (n)

illustrated in sketch (o). Clearly, these types of operation may no longer be considered as minimum time switching. Two approaches for remedying these problems will be considered next.

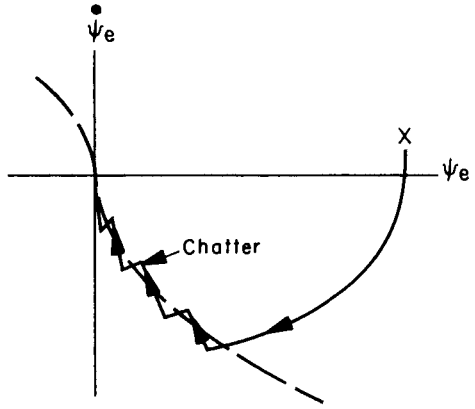


Sketch (o)

Switching curve approach.- On the basis of the above discussion, the position may be taken that the nonoptimum switching occurs because the switching line is insensitive to the system torque capability. If the switching function could take into account the variation in torque magnitude, then the system would switch at the time corresponding to minimum settling time. Proceeding with this idea, equation (50) for the switching function is put in the more convenient form:

$$\epsilon = |T_1|\psi_e + \frac{I_z}{2}\dot{\psi}_e|\dot{\psi}_e| \qquad (55)$$

In this equation the torque magnitude $|T_1|$ becomes one of the system variables. This torque magnitude may be determined by measuring the instantaneous wheel speed and relating this to a knowledge of the torque speed characteristics of the particular motor. The controller using this type of compensation is shown in sketch (p).

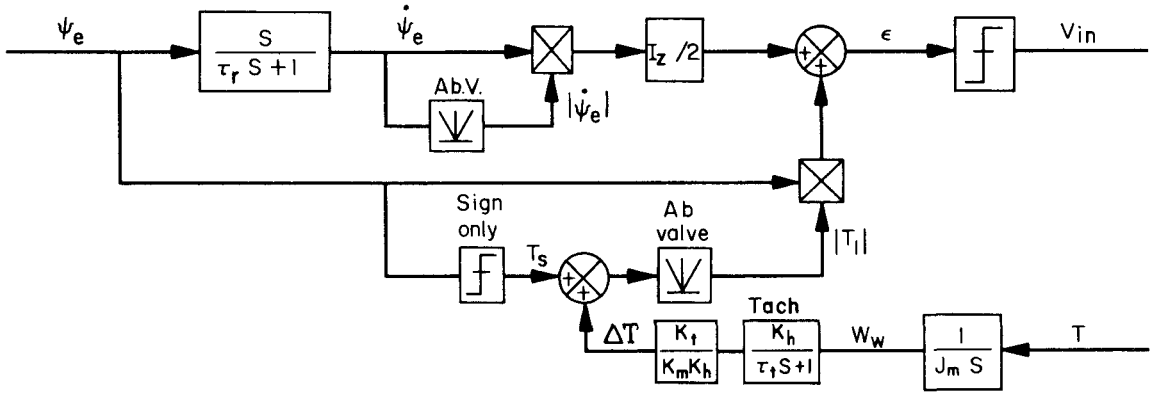


Sketch (p)

As the sketch shows, the available torque is determined by a tachometer which measures the wheel speed. The magnitude of this torque is obtained and multiplied by $\psi_e$. This product is added to the product of $\dot{\psi}_e$ and its magnitude to give the control function. The torque $|T_1|$ appearing here is not the instantaneous torque level of the system, but is the level that would be present if the function switched at any instant. In this sense, this function acts as an anticipator and continually adapts the switching curve to correspond to the torque level that will be present when the control function switches sign. This nonlinear controller will be referred to as the variable switch curve or V.S.C. controller.

Time constant approach: One other approach will be presented which compensates for the decay in torque output of the motor. For this method the tachometer is used in an inner loop around the torque motor. The tachometer

output is calibrated and used to control the level of the torque motor input voltage in such a manner that the output torque will be a constant throughout the operating speed range. The motor would have effectively a time constant of infinity. Sketch (q) shows a block diagram of the mechanization and torque-speed curves for the motor. Essentially, the tachometer is used to compensate for the back emf of the motor by adding to the input voltage an amount equal to the back emf. It should be realized that since the voltage to the motor must not exceed a specified maximum value, then the total input voltage, $V_{in} + V_{emf}$, will be less than the maximum value for wheel speeds less than $W_{w_{max}}$. This means that the motor does not produce "maximum available torque" at any time except at the extremes of the operating range. Sketch (q) shows the two curves for the maximum available torque and the actual output torque for the motor. The approach would not be considered an efficient way of using the motor even though the scan system incorporating the approach possesses favorable characteristics as will be demonstrated in a later section. The switch function of equation (50) would be applicable with this scheme which will be designated "nonlinear controller ($\tau_m = \infty$)" in the remainder of the paper.

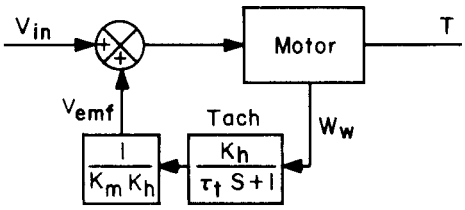


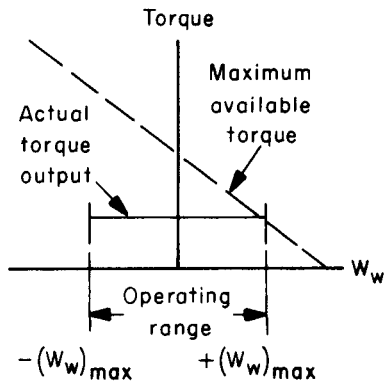


Sketch (q)

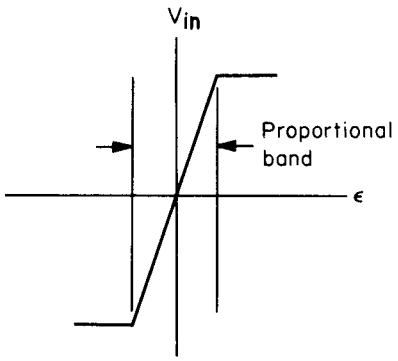


Sketch (r)

Dual-mode controller.- The system incorporating the controllers considered thus far has had objectionable characteristics that cause either overshooting, limit cycling, chattering, or a combination of these effects. A controller will now be considered which combines some of the better features of each of the others while eliminating the objectionable ones.

To the basic nonlinear controller, a region of proportional control is added which will be effective in the vicinity of the switching lines. The normal bang-bang element is replaced by a narrow proportional band amplifier with limiting characteristics as indicated in sketch (r). This linear region will produce a smooth torque reversal, eliminating chattering around the switch line while permitting a region of damped linear operation to be added in the vicinity of the origin. This resulting controller is known as dual mode and is discussed in reference 8. The switching function is represented by

$$\epsilon = \psi_e + \frac{\dot{\psi}_e|\dot{\psi}_e|}{2T_{min}/I_z} + P\ sat\left(\frac{K_r}{P}\dot{\psi}_e\right) \tag{56}$$

The first order error rate term in this switching function will damp small amplitude oscillations. The magnitude of this term is limited to have negligible effect in comparison with the second-order rate term for large amplitude rate errors. The torque magnitude, $T_{min}$, in equation (56) is a constant and is equal to the minimum operating torque level for the system. The use of this value will give a shallow switching curve which will correspond to the shallowest terminal trajectory for the system. Under this condition once a vehicle trajectory entered the proportional region it could not exit and overshoot the origin. The controller would appear as in sketch (s). The operation of this

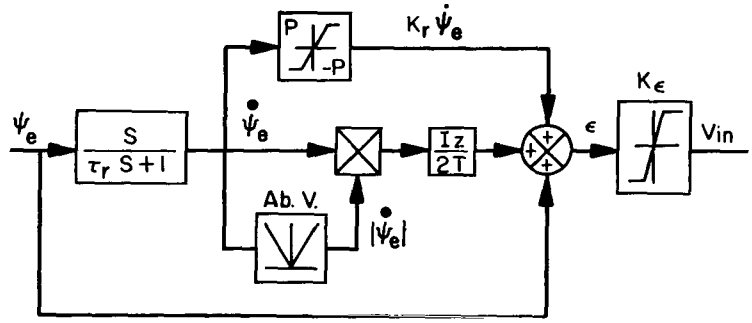


Sketch (s)

system will be explained with the aid of sketch (t). The switching function will have three distinct types of operation. In region ① the error signal $\epsilon$ will be large and will saturate the narrow band amplifier. The output $V_{in}$ will drive the torque motor at maximum available torque. This control voltage will be:

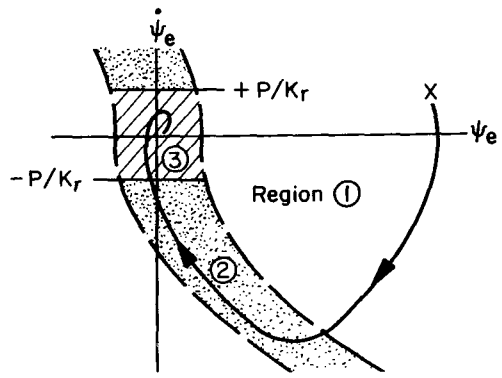


Sketch (t)

$$V_{in} = V_{max} \text{ sign } K_\epsilon \epsilon$$

In this region the trajectory motion will be the same as that for a system with the basic nonlinear controller. When the trajectory enters region ② the magnitude of the error signal will be within the proportional band of the amplifier. There will be a smooth variation in the error signal and a resulting smooth transition in the sign of the control torque. The first-order rate term of the switching function will be saturated and the control voltage will be the form:

$$V_{in} = K_\epsilon\left(\psi_e + \frac{\dot{\psi}_e|\dot{\psi}_e|}{2T_{min}/I_z} \pm P\right) \qquad (57)$$

The operation in region ③ is quasi-linear. The second-order rate term of the switching function will have negligible effect and the control voltage may be approximated by equation (58).

$$V_{in} = K_\epsilon(\psi_e + K_r\dot{\psi}_e) \qquad (58)$$

The system operating in this region will damp any oscillation and thus eliminate the limit cycle which is characteristic of the nonlinear systems.

## ANALOG COMPUTER SIMULATION

A simulation was made of a system with the various controllers on an analog computer. The operational characteristics of the system were first determined and then a performance comparison was made with the different controllers. The various components of the simulated control loop are presented in block diagram form in figure 2. There will be a total of five variations of this system under consideration. The differences come about as a result of changes in the controller. The components of the remainder of the loop are not changed. Details of the controllers were presented in sketches (f), (l), (p), (q), and (s) for the linear, nonlinear, nonlinear variable-switching curve, nonlinear ($\tau_m = \infty$), and the dual-mode controllers, respectively.

As an example for this study the vehicle inertia characteristics and the specifications for the scan control system for the Advanced Orbiting Solar Observation (AOSO) will be used to determine the control-system parameters. The entire AOSO vehicle ($I_z = 2.03 \times 10^9$ g-cm$^2$) is required to scan a 40 arc-min square area with 120 scan lines in a total time of 30 minutes. The maximum scan rate may not exceed 3.6 arc-min/sec and the absolute pointing error may be no greater than 5 arc-sec. Jitter in pointing is limited to ±1 arc-sec, with a maximum rate of jitter not to exceed ±0.5 arc-sec/sec.

From these specifications the maximum time available for vehicle turnaround may be determined to be about 3.89 sec. A corresponding average value of turnaround torque to complete the maneuver within this time would be approximately $1.1 \times 10^6$ dyne-cm. This value would represent the minimum acceptable average torque magnitude. Since the torque is not constant but decays with time, it requires that the initial and final magnitudes be different from this average value. These values will be a function of the stall torque and the operating range of the motor. For the purpose of this study, a stall torque magnitude of $3.39 \times 10^6$ dyne-cm (0.25 ft-lb) was selected. An operating range which corresponds to a momentum capacity of $\pm 1.36 \times 10^7$ dyne-cm-sec (1 ft-lb-sec) is large enough to absorb the momentum exchange of the turnaround and has been shown by previous studies to be adequate for absorbing the external disturbances expected for the AOSO vehicle. This range is selected and corresponds to a motor time constant of 7 sec. For convenience, the inertia wheel speed of 100 radians/sec will be equivalent to a momentum of $1.36 \times 10^7$ dyne-cm-sec; thus $J_m = 1.36 \times 10^5$ g-cm$^2$ (0.01 slug-ft$^2$). Note that the extremes of this operating range do not correspond to torque motor saturation but to the point at which minimum operating torque level is realized. Thus, if a turnaround is initiated with a wheel speed of 100 radians/sec, the turn will be accomplished in 3.89 sec (the maximum available turnaround time) with an average control torque of $1.1 \times 10^6$ dyne-cm.

A determination will now be made of the various gains which correspond to the proportional region of the linear and the dual-mode controller. The

natural frequency is related to the acceptable steady-state tracking error as given in equations (14), (15), and (16). For the condition of a saw-tooth ramp command, an initial wheel speed but no disturbance torques, the steady-state error equation will be the sum of equations (16) and (18). Rearranging and expressing the system frequency in terms of the steady-state error gives

$$\omega_n^2 = \frac{1}{\tau_m \psi_{e_{ss}}} \left( \dot{\psi}_c + \frac{J_m}{I_z} W_{w_o} \right) \tag{59}$$

Of course, this equation could be obtained directly by applying the final value theorem to equation (9) for the initial condition stated. Evaluating equation (59) at the extreme of the torque motor operating range (100 radian/sec) for an error of 5 arc-sec with maximum scan rate gives a system frequency of 6.74 radians/sec.

For a damping ratio of 0.7, equation (12) is evaluated to give a rate gain for the controller of $K_r = 0.2045$ V/arc-min/sec. To evaluate the gain $K_\epsilon$ for the proportional zone of the limiter, it is necessary to specify a maximum motor input voltage. For maximum $V_{in}$ of 28 V, $K_t = 1.21 \times 10^5$ dyne-cm/V, and by combining equations (10) and (11), and the definition of the motor time constant, $\tau_m = J_m K_m / K_t$, $K_\epsilon$ may be found as:

$$K_\epsilon = \frac{\omega_n^2 I_z}{K_t} \tag{60}$$

Evaluating this expression gives $K_\epsilon = 222$ V/V.

With the evaluation of these gains the characteristics of the system are defined with the exception of the sun sensor. The dynamics of this component have been ignored thus far. A basic design criteria for this type sensor requires a bandwidth of approximately 40 radians/sec (ref. 3). This is considered fast in comparison with the control system frequency. The output of the sun sensor is not limited in the range of the attitude variable change, and for these reasons the transfer function is essentially unity and is neglected in the study.

## RESULTS AND DISCUSSION

The results of the analog computer study will be presented in three phases. The initial discussion will be concerned with the scan phase in which the system with each of the five controllers will be examined for response to a step error input and torque disturbances. A second phase will present the results of the simulation of the turnaround maneuver with the five mechanization schemes examined. Finally, the complete raster scan maneuver is examined in which the two phases are combined into the complete system.

## Scan System Error Response

The performance of the systems for large initial errors in position pointing is shown in figures 3(a) through 3(e). An initial error of the magnitude shown (3 arc-min) is large in comparison to the acceptable pointing error (5 arc-sec) but is of the size which could result from an inefficient turnaround maneuver. The initial rate error and rate command are both assumed to be zero. Presented in figure 3(a) are typical phase-plane trajectories for the system with the linear controller. In addition, the corresponding transient response curves are shown. The three trajectories in each plot represent the vehicle recovery from the pointing error with three different initial torque-motor wheel speeds, -50, 0, and +50 radians/sec (50 radians/sec corresponds to 50 percent of the allowable operating range). An obvious trajectory overshooting problem is encountered for this system. In general, for initially positive errors the overshoots and transient times are increased for initially positive wheel speeds because the magnitude of control torque is lower. The opposite occurs for initially negative wheel speeds where higher torque is driving the system.

The extent of the overshooting is also dependent on the slope and width of the proportional zone, but as demonstrated in a previous section, these factors are specified by the natural frequency and damping characteristics desired within this zone. The proportional zone is shown as the shaded region in the phase-plane plot.

The characteristic motions of the system with the basic nonlinear controller are shown in figure 3(b). The switching curve presented in the phase-plane plot is selected to correspond to the terminal trajectory which would result from operating at the stall torque level of the control motor. As predicted in the analysis section, overshooting of the origin occurs when the system is operating at torque levels less than this stall torque value. The other undesirable effects are present too. Chattering is apparent in the phase plane when the system operates at a torque level higher than the stall torque. The trajectory motion will always terminate into some degree of limit cycle operation in a real system due to the presence of hysteresis effects and component time lags.

The operation of the system with the nonlinear variable switching curve controller is shown in figure 3(c). It is apparent from the phase-plane representation that the shape of the switching lines has changed for each of the three trajectories in the figure. This change is due to an automatic adjustment of the gains of the switching network so as to shape the switching curve to correspond with the trajectory at the different torque levels. The torque level is obtained by measuring the instantaneous inertia wheel speed and relating this to the torque capability through a knowledge of the torque-speed curve.

The three trajectories in figure 3(c) show an apparent improvement in performance in terms of smoothness of operation, overshooting, and transient times. In the phase-plane plot the tendency to overshoot the origin has completely disappeared. The chattering, which comes from an undershooting

tendency, has also been eliminated. The time response plots show that the transient times are essentially equal for all three initial wheel speed condi-conditions.

The other method presented in the analysis for compensating for torque decay problems was termed "the time constant approach." In this method the tachometer output is used to adjust the motor input voltage so that the output torque will remain constant. This type of operation would correspond to that of a torque motor with an effective time constant of infinity. Figure 3(d) shows the response of the system with the nonlinear controller for this type of compensation. The shape of the trajectories will no longer vary with wheel speed; thus, they appear as only one trajectory in the figure. The time response of the system is about equal to that for the variable switching curve (V.S.C.) approach. In order for the time responses of the two systems to be equal, it was necessary to assume a motor for the "time constant scheme" ($\tau_m = \infty$) with a constant torque output equal to the stall torque value of the motor used with the V.S.C. controller. As a result, the stall torque rating of the motor for the ($\tau_m = \infty$) scheme is about 60 percent higher than that used with the V.S C. scheme. This means that a larger motor was needed to give equivalent performance. It is interesting that although the response of this system is fast, it is no faster than the more efficient variable switch curve scheme even though it requires a larger torque motor. Unfortunately, the system with either nonlinear controller has the undesirable characteristic of a terminal limit cycle in the region of the origin in the phase plane. The magnitude of this limit cycle or jitter rate would make all three nonlinear systems unacceptable under the criteria specified for the advanced OSO vehicle.

The performance of the system with the dual-mode controller is presented in figure 3(e). The switching curves were chosen to correspond to the terminal trajectory for the minimum operating torque level of the system (at $W_{W_O} = 100$ radian/sec). The gains for the quasi-linear region ($K_\epsilon, K_r$) were equivalent to those calculated for the linear saturation system. It is apparent from the figure that there is no tendency for the trajectories to overshoot the origin. The limit cycle problem of the nonlinear controllers is not present, and there is no tendency toward chattering in the vicinity of the switching lines. In the switching zone, there is a gradual reversal of the control torque magnitude which is favorable from the standpoint of motor reliability. The appearance of the trajectories on the transient response plot indicates that the system is slightly overdamped. A faster system could be achieved with the choice of a more suitable set of gains for the proportional regions.

The effect of a large torque disturbance can be seen from the computer runs for the system with the various controllers presented in figure 4. For zero initial wheel speed, the performance of each of the systems is adequate with respect to holding the mean pointing direction within the 5 arc-sec criterion. A small increase in pointing error is apparent after the disturbance has been damped. This is due to an increase in inertia wheel speed resulting from the exchange of momentum. The magnitude of the steady-state error may be determined from equation (15) of the analysis section. The response with the dual mode and linear controller is quite similar as is that for the system with the nonlinear controllers. The "jitter" in pointing due to the nonlinear controllers is more apparent in this figure than in the previous ones. In the

right half of figure 4, the effect of an increase in the initial wheel speed may be seen. The steady-state tracking errors are larger for the linear and dual mode case by the amount predicted in equation (16). The effect of wheel speed for the nonlinear case is to increase the amplitude of the jitter and decrease the frequency. There is also a corresponding increase by a factor of 2 in the magnitude of the error in response to the same torque disturbance.

The graph in figure 5 presents a comparison of the large signal error response for the system with the linear controller with that for the system with the dual-mode controller. The transient time for the dual-mode case is less throughout the range of initial position error. The system for this case demonstrates distinctly faster response for the larger initial errors. At these large values, the performance is comparable with a minimum time switch curve system which is represented by the dashed line in the figure. This line corresponds to the values calculated from equation (53). The other dashed line, designated "linear switch curve," was determined by the method presented in the text. These values of total response time result from the summation of the time increments as determined from equations (33), (38), (40), and (44) with the initial conditions of $\dot{\psi}_{e_o} = \dot{\psi}_c = W_{w_o} = 0$ and $\psi_{e_o}$ ranging from 0 to 5 arc-min. Although the response of the system with the dual-mode and linear controllers is quite different for large errors, the response times are nearly equal for small errors and almost identical for operation within the proportional region.

## Turnaround Performance

The results of the computer study of the various schemes for generating the command for the vehicle turnaround are presented in figures 6(a) through 6(e). The various schemes are demonstrated in conjunction with a scan system incorporating the dual-mode controller although the particular type of controller used will have no direct effect on the performance during the turnaround. The figure shows the vehicle attitude and the attitude error signal as a function of time. As a basis for comparing performance among the various cases, the attitude error is defined relative to a simple sawtoothed command signal in all cases rather than the actual system command input. In this way the attitude error for the various systems may be compared directly.

Figure 6(a) shows the response of the system to the simple sawtooth command. It is apparent that the system will not follow this signal during the turnaround. The result is a large overshoot for each of the three runs which correspond to three different initial wheel speeds at the start of the maneuver. Also, note that half of the turnaround time available prior to the apex of the sawtooth has not been used.

The performance of a position limited command signal scheme is presented in figure 6(b). Although the approach makes use of more of the available time, there are still large overshoots for operation at positive wheel speeds where the available control torque is less than the mean level for which the system would be designed. Also present in this system is the characteristic designated in the analysis section as "undesirable switching." This is apparent in that attitude error curve which corresponds to operation with an initial wheel

speed of -50 radians/sec. Note that the curve tends to flatten out and become parallel with the zero attitude error axis about halfway through the turnaround. This indicates that the control torque has switched signs before the turn maneuver is complete. When the command signal is again a ramp, the system recovers and completes the maneuver within the allowable time.

The performance characteristics of a scheme which eliminates the overshoots from the first two cases are presented in figure 6(c). This system is the compensated position-limited command. The extent of the flattening for the command signal is variable and a function of the wheel speed. The turnaround maneuver is initiated at different times so as to achieve a smooth transition into the scan phase at the end of the turnaround. The smoothness of this system operation is apparent in figure 6(c). The system has an undesirable switching tendency, as may be seen in the attitude error trace for $W_{w_o} = 0$.

The two other schemes studied are open-loop command systems. The systems operations are shown in figures 6(d) and 6(e). In both schemes the loop is opened at a specified position outside the useful scan region. For the operation shown in the figures, this position is approximately 25 arc-min. An external signal energizes the torque motor, producing the maximum available control torque throughout the open-loop portion. The loop is closed in the first case (fig 6(d)) at a preselected vehicle attitude position. The position should be within the range from the apex of the sawtoothed command signal to the attitude at which the loop was open (25 arc min). The performance of the system is not sensitive to the exact value.

For figure 6(e) the loop was closed when the vehicle attitude rate was equal to the command rate. Thus the time of loop closing is variable as indicated in the figure.

It is apparent that neither of the open-loop approaches produces the type of performance that is desired. From a comparison of the performance of each of the five schemes it may be stated that the "compensating position-limited" command input shown in figure 6(c) comes closest to achieving the desired smoothness during the turnaround maneuver of the spacecraft.

## Complete System

As the final phase of the analog computer study, a complete raster scanning maneuver was studied. The two phases of the maneuver which have been examined separately up to this point in the report are combined into the complete system. The results of this study showing the dynamics of five different complete line-scanning systems (different controllers only) with the same turnaround system are presented in figures 7(a) through 7(i). The turnaround system in each case will be the compensated position-limited command scheme.

The attitude error is again determined relative to the basic sawtoothed signal. Runs are presented for operation around zero wheel speed and also for an initial wheel speed of 50 radians/sec.

It seems unnecessary to discuss each of figures 7(a) through 7(i) in detail. Instead, a summary of all nine figures will be presented.

Initially, it may be stated that each of the systems discussed is a practical raster scan system. It is also apparent that the assumption made initially, that the maneuver may be divided into two phases, each examined separately and then later combined, is verified by the result present here. Each of the systems track the scan command with a mean error within the specified 5 arc sec. This value cannot be verified on these figures but only because of the scale for which the traces were recorded. Each of the turnaround maneuvers is completed within the allowable time of 3.89 sec. The same problem encountered before is apparent for the system with each of the nonlinear controllers. In each case the rate error (jitter rate) is in excess of the allowable value, making the system unacceptable. The general character of the operation of the linear and the dual-mode cases is quite similar as seen in figures 7(a), 7(b), 7(h), and 7(i). The system, with either of these controllers, would be acceptable under the criteria as presented for the advanced OSO spacecraft.

Tables I and II present summaries of the performance of the various systems. Table I summarizes the scan performance of each case analyzed for the design criteria outlined earlier. This summary shows that the five variations of the scan system have comparable and acceptable performance for all stated criteria except one. The jitter rate for each of the nonlinear cases, as stated previously, is far in excess of the allowable (±1/2 arc-sec/sec). These three cases would not be acceptable for the high resolution scan desired.

From the turnaround performance (table II), it is apparent that the compensated position-limited system outperforms the four other approaches. Over the range of wheel speed used, this was the only system which could perform the turnaround consistently within the allotted time (3.89 sec). If reference is made to figures 5(a) through 5(e), it also appears that this is the only approach examined which gives a smooth, efficient, and repeatable turnaround.

## SUMMARY OF RESULTS

The performance of several variants of a satellite control system for scanning a small celestial area has been investigated. The control torque was supplied by an inertia wheel in combination with a torque motor. The scan system was analyzed on the basis of tracking accuracy, recovery from large disturbances, and effects of inertia wheel momentum build-up. The turnaround phase was studied with the objective of obtaining a smooth and efficient reversal of the vehicle scan velocity.

1. A large variation in system behavior is encountered for both the scan and the turnaround phases as a result of inertia wheel momentum. For adequate performance it is necessary to restrict the operational range of the inertia wheel.

2. Adequate response to initial pointing errors up to 5 arc min and torque disturbance of $1 \times 10^6$ dyne-cm could be obtained from the scan system for each of five types of controllers investigated. Mean tracking errors were less than 5 arc sec in all cases.

3. The scan system incorporating either of the three nonlinear controllers exhibited undesirable characteristics (jitter or jitter and chatter) and are unacceptable because of this behavior. The linear and the dual-mode controller incorporated a region of proportional control in the vicinity of the origin and switching line. This region eliminated the tendency to jitter and chatter. Thus, the system with either the linear or dual-mode controller is acceptable for the high precision scanning that is required.

4. The turnaround performance of the system was found to be acceptable only when the mechanism for generating the turnaround command signal was modified to adapt to changes in the control torque level due to inertia wheel momentum build-up. When this was done, a smooth and efficient turnaround was obtained.

Ames Research Center
National Aeronautics and Space Administration
Moffett Field, Calif., May 25, 1966

## APPENDIX A

## TORQUE MOTOR TRANSFER FUNCTION

A combination ac servomotor and inertia wheel is assumed to be the control torque source in this study. The ac servomotor is a two-phase induction motor. To one of the motor windings a constant amplitude voltage is applied. The voltage to the other winding is varied and the torque and wheel speed is a function of this voltage. A set of torque speed curves for various magnitudes of the control input voltage would appear as in sketch (u). Generally, the torque speed curves are not straight lines but the assumption of linearity simplifies the transfer function considerably and is a good approximation for the actual variations. If the curves are assumed to be equally spaced straight lines the form of the torque equations would be

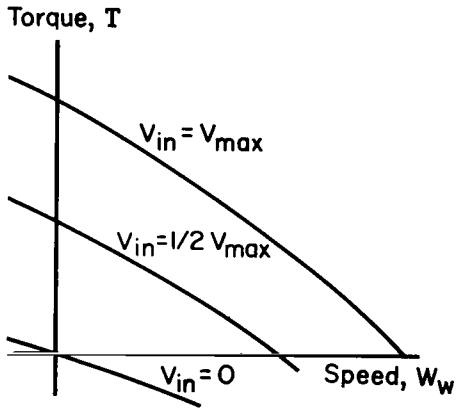


Sketch (u)

$$T = \frac{\partial T}{\partial V_{in}} V_{in} + \frac{\partial T}{\partial W_w} W_w \qquad (A1)$$

where the torque output, T, is a function of the wheel speed $W_w$ as well as the input voltage $V_{in}$. Under the linearity assumptions the partial derivative coefficients will be constant and the equation may be transformed directly to the S domain. In terms of the parameters which will be used in this study, the equation (A1) becomes

$$T(s) = K_t V_{in}(s) - \frac{K_t}{K_m} W_w(s) \qquad (A2)$$

The negative sign of the coefficient $K_t/K_m$ results from the negative slope of the torque speed curves. From elementary mechanics, the torque may also be defined as the time rate of change of angular momentum. In terms of the transform variable this expression would be

$$T(s) = J_m S W_w(s) - J_m W_w(0) \qquad (A3)$$

where $J_m W_w(0)$ is the value of the momentum at time equal zero. For convenience, $W_w(0)$ will be designated $W_{w_o}$ hereafter. By combining equations (A2) and (A3), eliminating $W(s)$ and rearranging terms, we obtain a useful expression for the control torque

$$T(s) = K_t\left(V_{in} - \frac{W_{w_o}}{K_m S}\right) \frac{\tau_m S}{\tau_m S + 1} \qquad (A4)$$

where

$$\tau_m = \frac{J_m K_m}{K_t}$$

Equation (A4) is the torque motor transfer function presented as equation (1) in this report.

## REFERENCES


1. Cervenka, Adolph J.: One Approach to the Engineering Design of the Advanced Orbiting Solar Observatory. NASA SP-30, 1963.

2. White, John S.; and Hansen, Q. Marion: Study of Systems Using Inertia Wheels for Precise Attitude Control of a Satellite. NASA TN D-691, 1961.

3. Cantor, Clarence: Fine Sun Tracker for Advanced Orbiting Solar Observatory. Proc. 10th Annual East Coast Conference on Aerospace and Navigational Electronics, Oct. 21-23, 1963. Western Periodicals, North Hollywood, 1963, pp. 1.5.4-1 to 1.5.4-10.

4. Schmidt, Stanley F.: The Analysis and Design of Continuous and Sampled-Data Feedback Control Systems With a Saturation Type Nonlinearity. NASA TN D-20, 1959.

5. Maxwell, David J.: Time Optimal Control of Second Order Systems. Fourth Joint Automatic Control Conference, Am. Inst. Chem. Engr., N. Y., June 19-21, 1963, preprints of technical papers, pp. 219-230.

6. Brown, Stuart C.: Predicted Performance of On-Off Systems for Precise Satellite Attitude Control. NASA TN D-1040, 1961.

7. Lewis, John B.: Optimum Response Relay Servos. Part 1: Evolution of the Optimum Switching Criteria. Control Engineering, May 1960, pp. 125-129.

8. Weed, H. R.; and Weimer, F. C.: A Dual-Mode Servomechanism Utilizing Saturation Switching. (Paper 58-1191), Trans. Am. Inst. Elec. Eng., vol. 77, pt. 2 (Applications and Industry), no. 40, Jan. 1959, pp. 590-595.

TABLE I.- SCAN PERFORMANCE

| System type / Design criterion | Linear | Nonlinear | Nonlinear (V.S.C.) | Nonlinear ($\tau_m = \infty$) | Dual mode |
|---|---|---|---|---|---|
| [1]Mean tracking error, arc sec | 2.5 | 1 | 1 | 0 | 2.5 |
| Jitter in position, arc sec | 0 | ±1.5 | ±1.5 | ±1.5 | 0 |
| Jitter rate arc sec/sec | 0 | ±24 | ±24 | ±24 | 0 |
| Chatter | no | yes | no | no | no |
| [1]Setting time, sec ($\psi_{eo}$ = 3 arc min) | 2.9 | 2.9 | 1.6 | 1.4 | 1.7 |
| [1]Torque response, sec | 1.7 | 1.1 | 1.3 | 1.1 | 2.1 |
| [2]Relative system complexity | 1 | 2 | 4 | 3 | 3 |

TABLE II.- TURNAROUND PERFORMANCE

| Command type / Design criterion | Sawtooth | Position limited | Compensated position limited | Open loop position sensitive closing | Open loop rate sensitive closing |
|---|---|---|---|---|---|
| Available time unused, sec | 1.9 | 1.3 | 0.9-1.4 | 1.3 | 1.3 |
| [1]Turnaround time, sec | 9.5 | 7.0 | 3.0 | 7.0 | 6.5 |
| [1]Max. terminal error, arc min | 8 | 3.5 | 0 | 4.8 | 2.5 |
| Undesirable switching | no | yes | yes | yes | yes |
| [2]Relative system complexity | 1 | 2 | 3 | 3 | 4 |

[1]$W_{w_o}$ = 50 radians/sec

[2]Higher numbers indicate more mechanization complexity

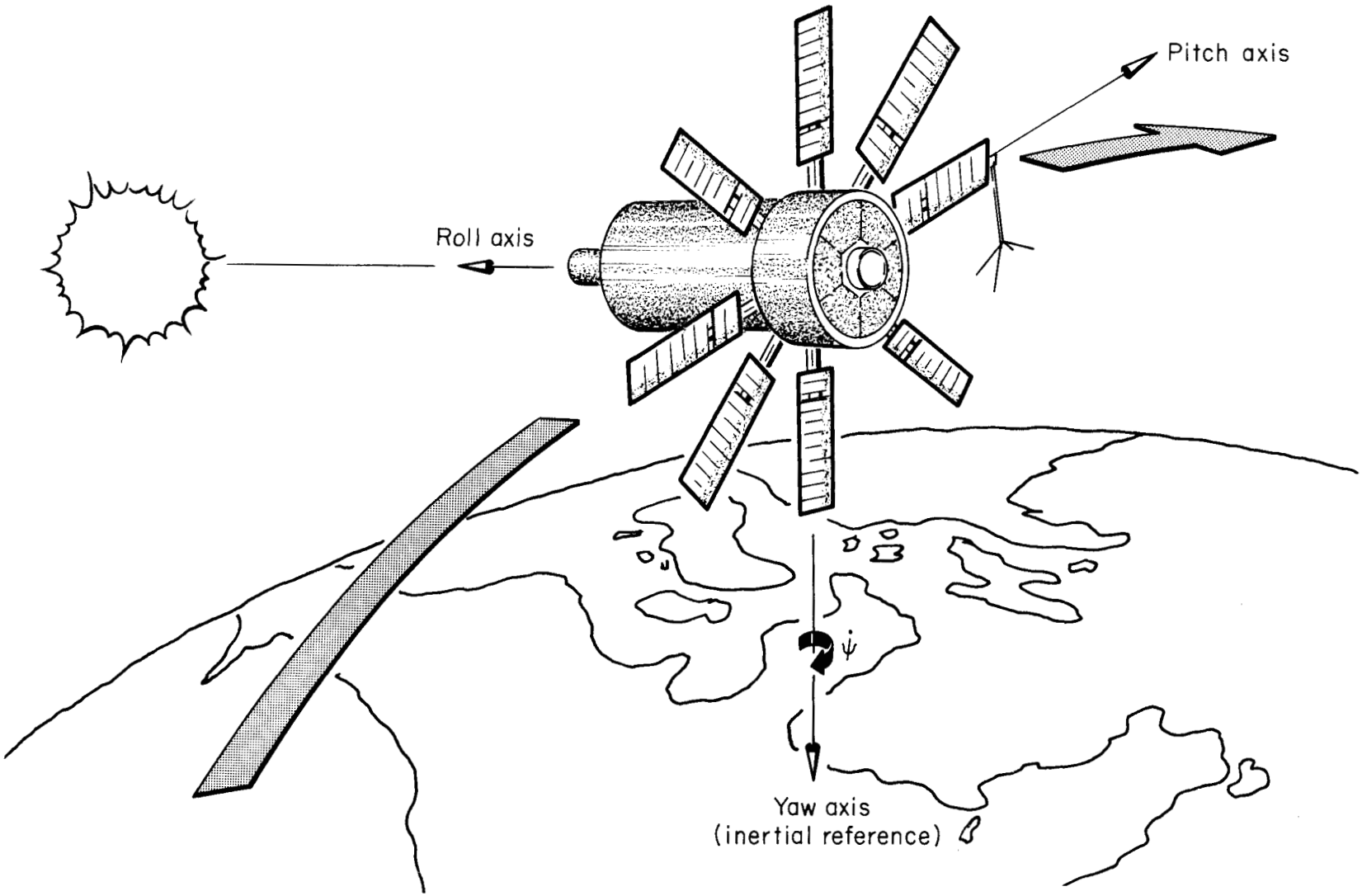


Figure 1.- Artist's conception of spacecraft performing raster scan operation.

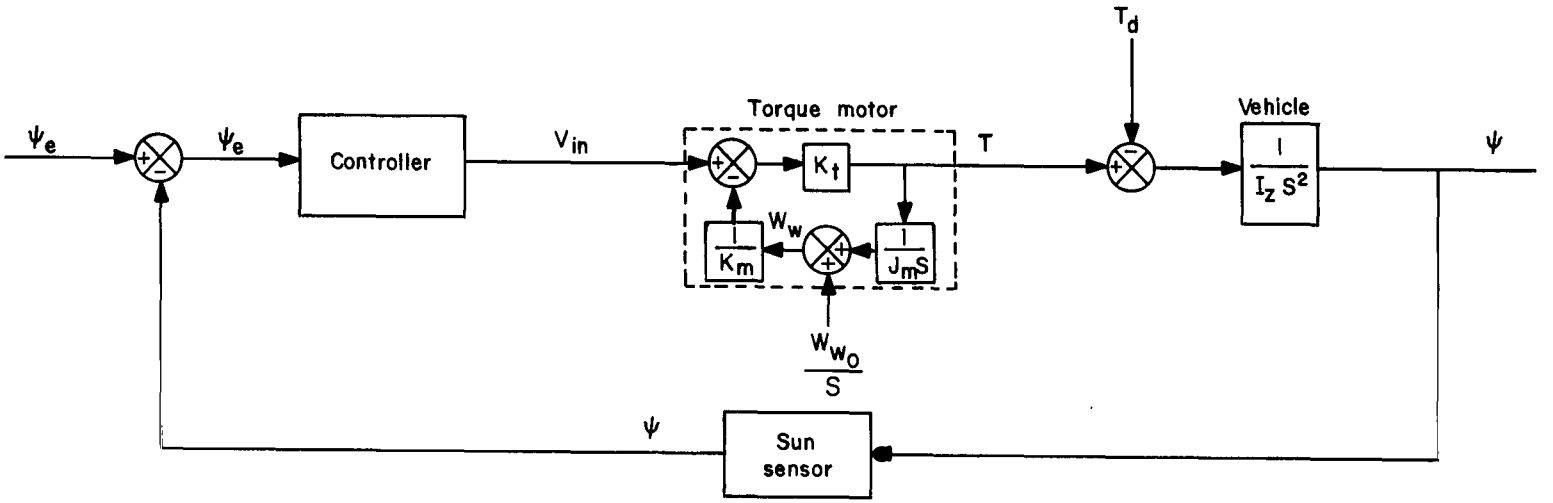


Figure 2.- Schematic block diagram of raster scan control system.

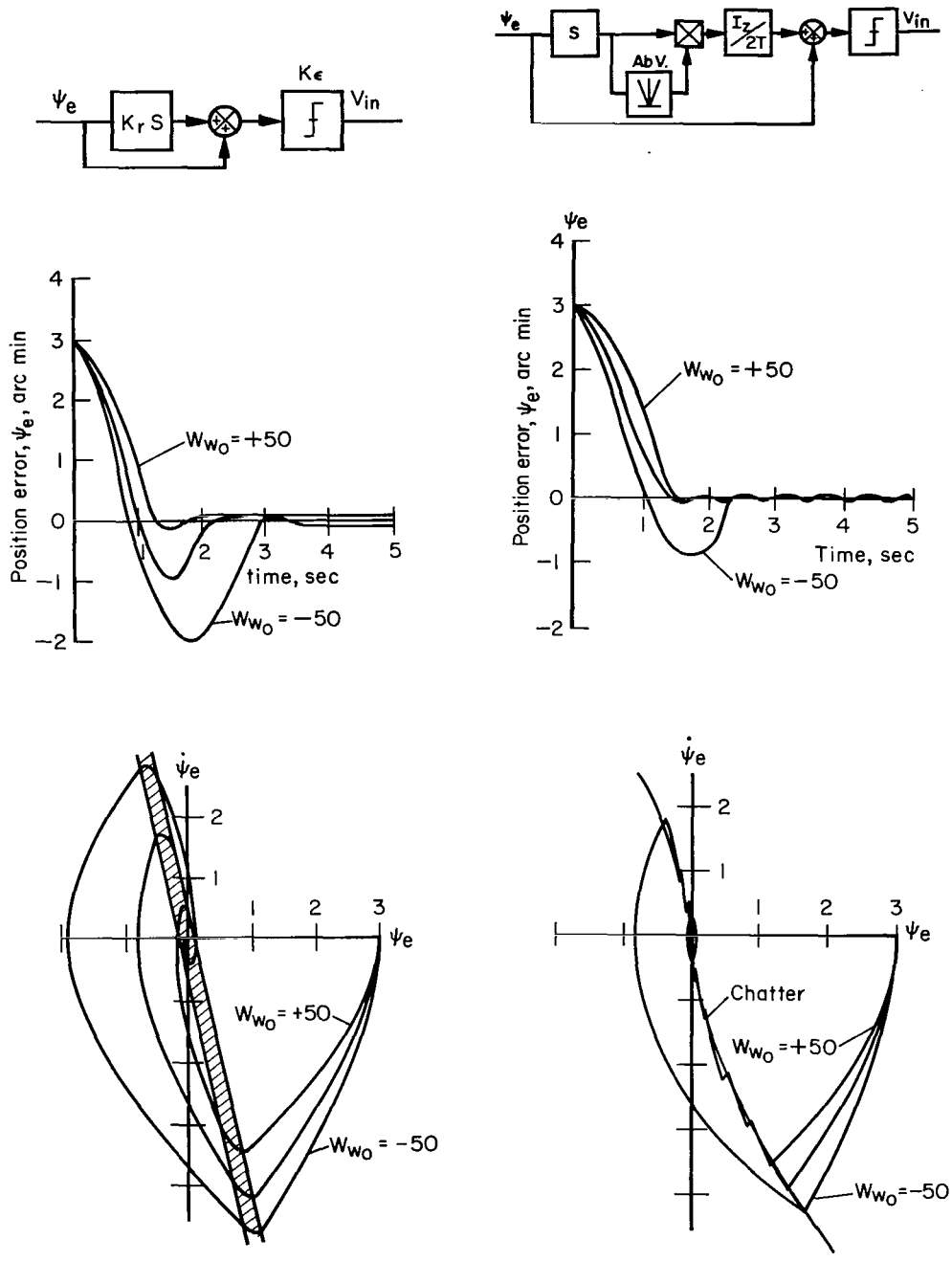


(a) Linear controller.

(b) Nonlinear controller.

Figure 3.- Response curves for position step input showing effect of initial wheel speed.

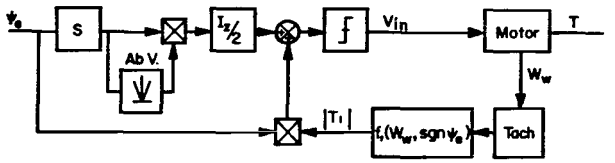


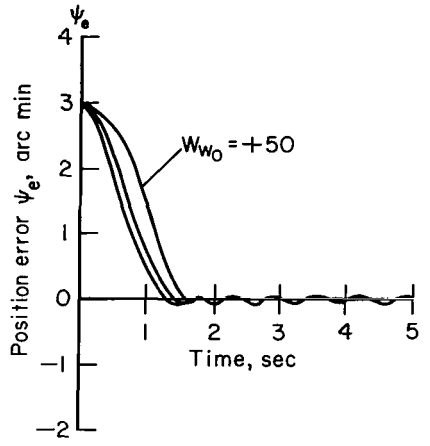


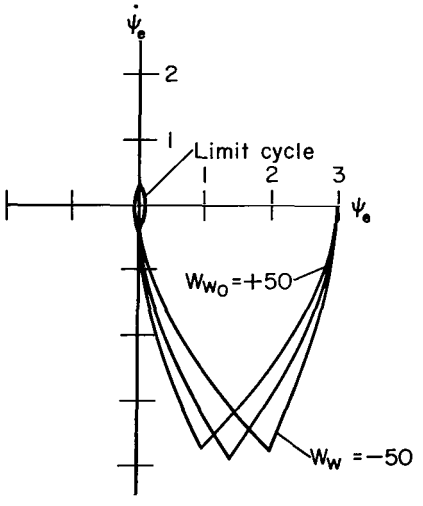


(c) Nonlinear controller (variable switching curve).

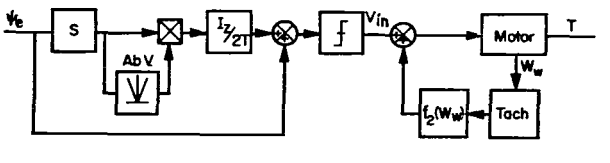


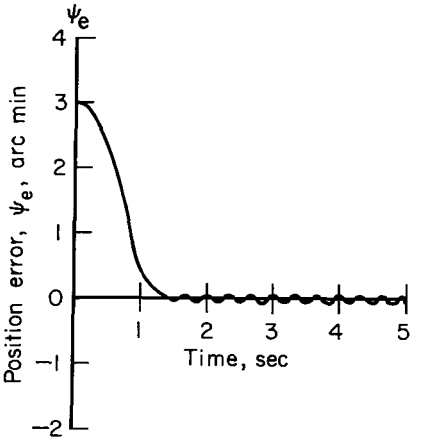


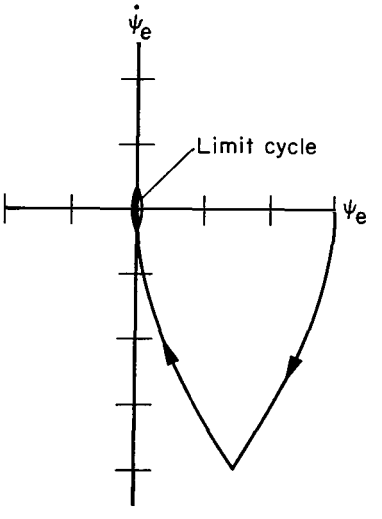


(d) Nonlinear controller ($\tau_m = \infty$) (time constant approach).

Figure 3.- Continued.

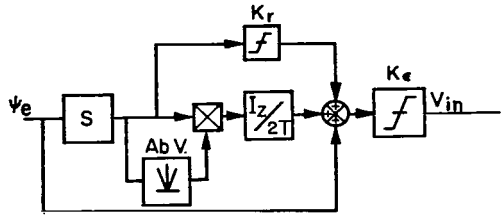


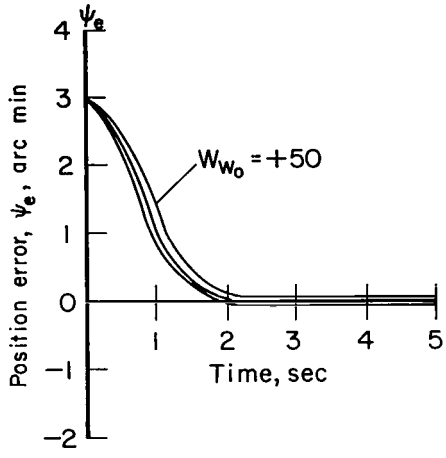


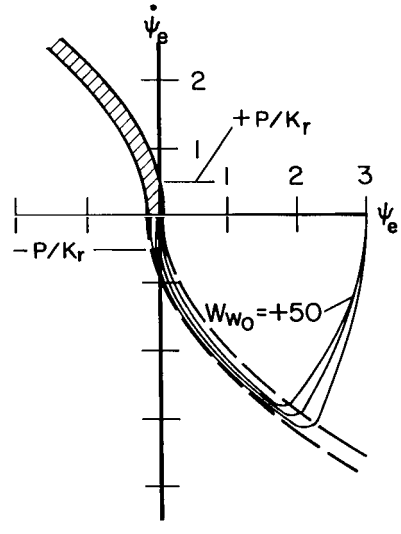


(e) Dual-mode controller.

Figure 3.- Concluded.

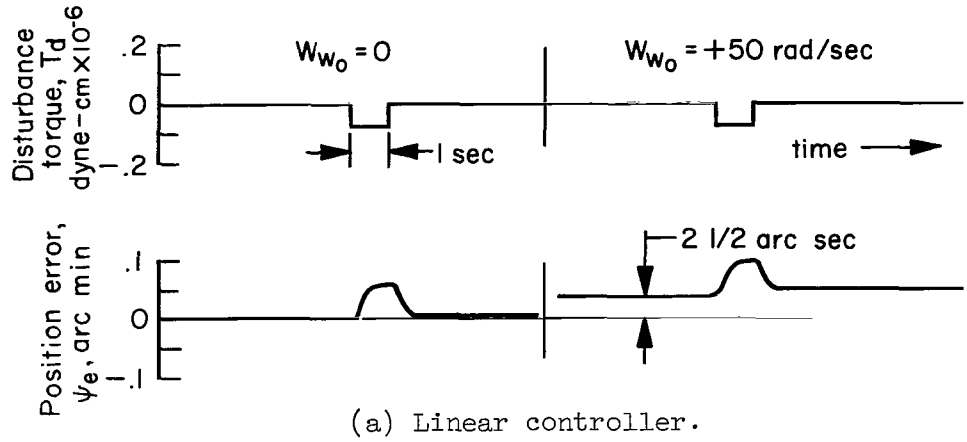


(a) Linear controller.

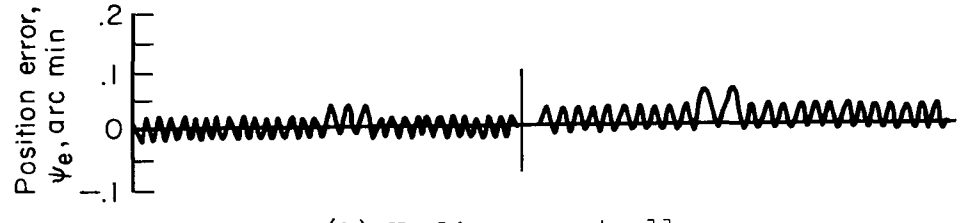


(b) Nonlinear controller.

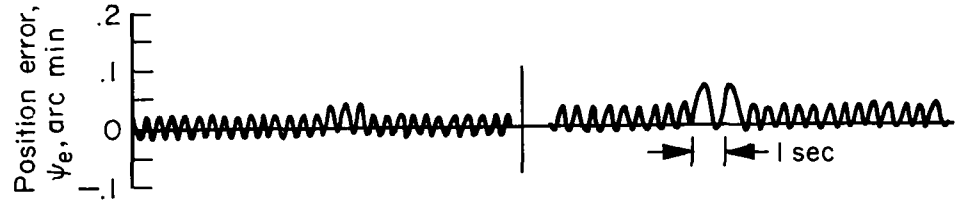


(c) Nonlinear controller (variable switch curve).

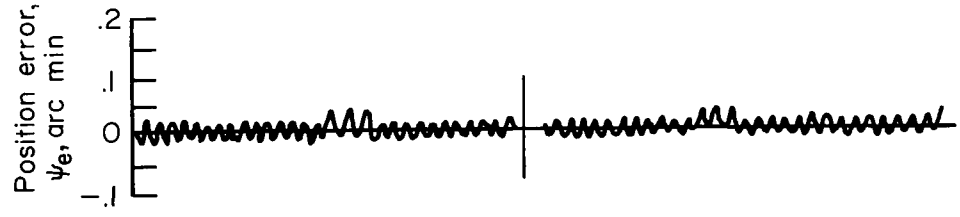


(d) Nonlinear controller ($\tau_m = \infty$).

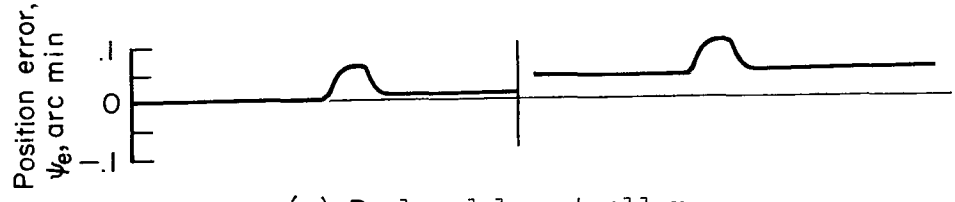


(e) Dual-model controller.

Figure 4.- Disturbance torque response showing effect of initial wheel speed.

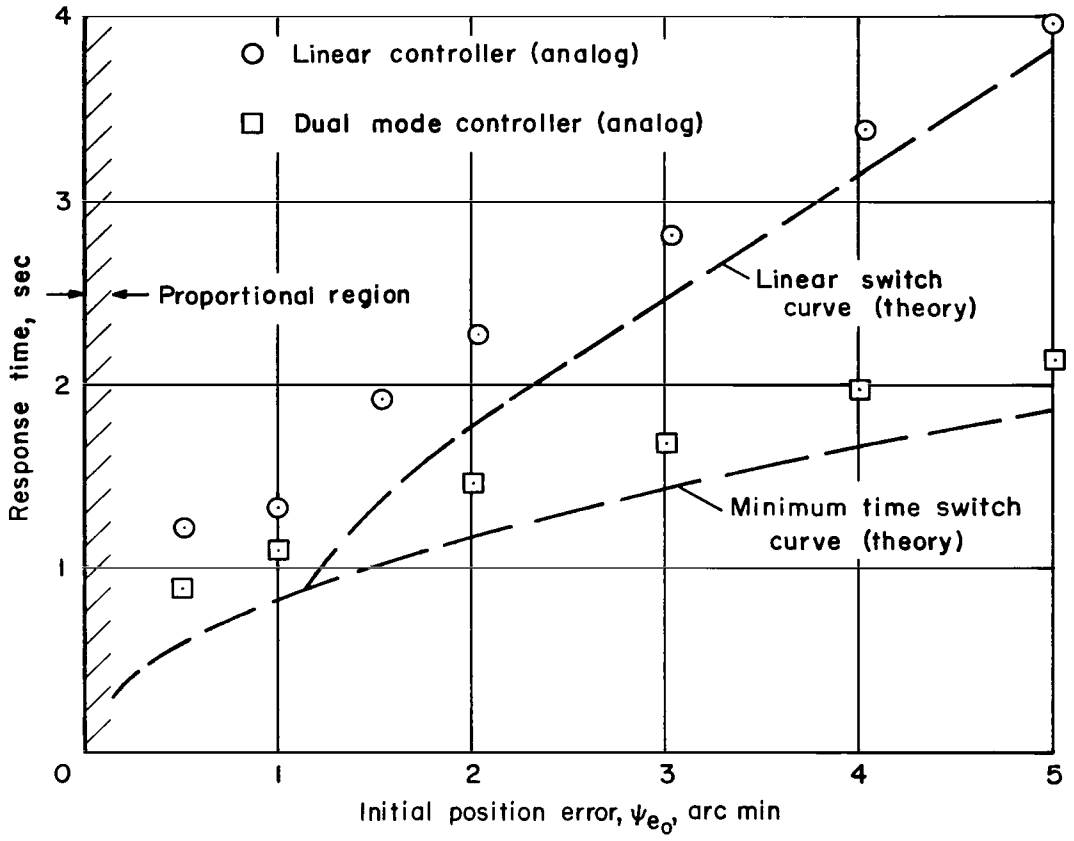


Figure 5.- Comparison of system response times for linear and dual-mode controllers ($W_{w_o} = 0$).

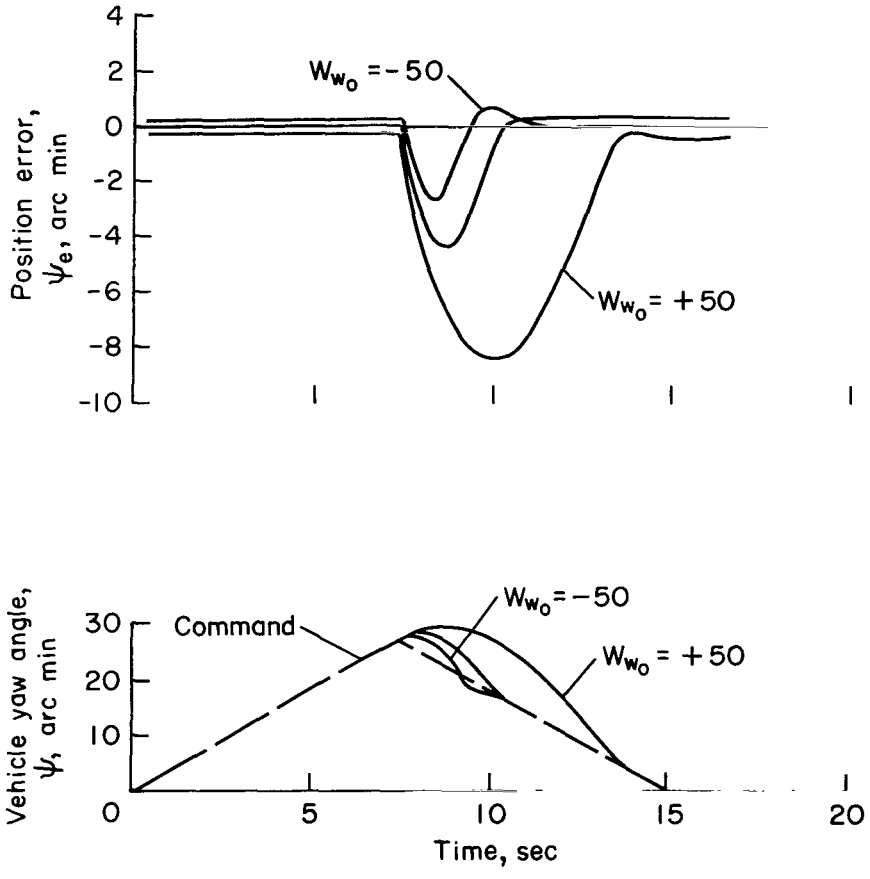


(a) Sawtoothed command.

Figure 6.- Turnaround maneuver showing effect of initial wheel speed (scan system with dual-mode controller).

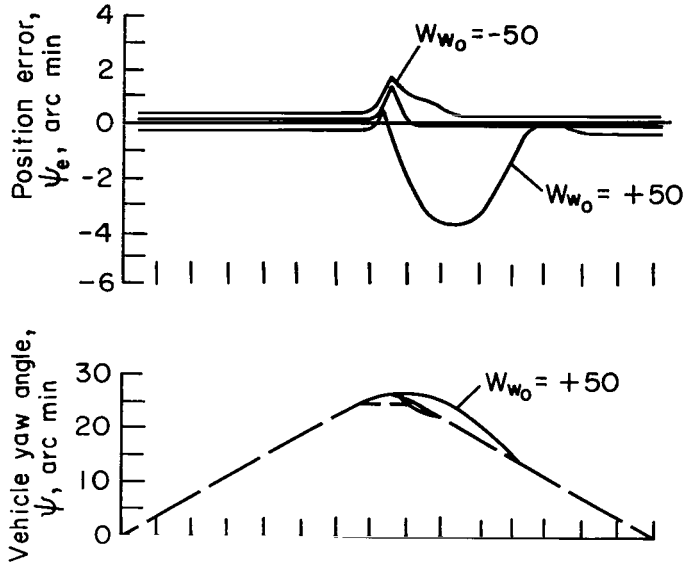


(b) Position limited command.

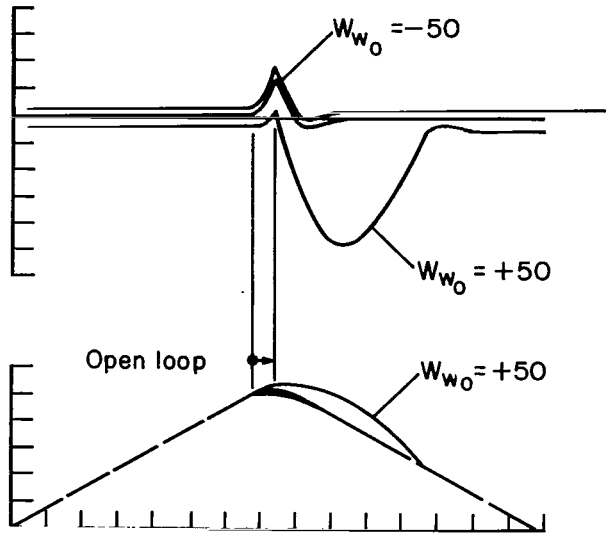


(d) Open-loop command (position sensitive loop closing).

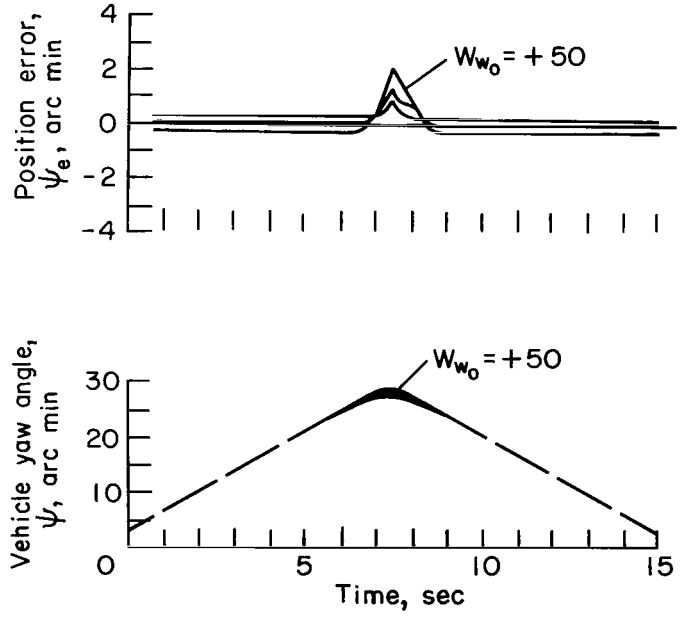


(c) Compensating position-limited command.

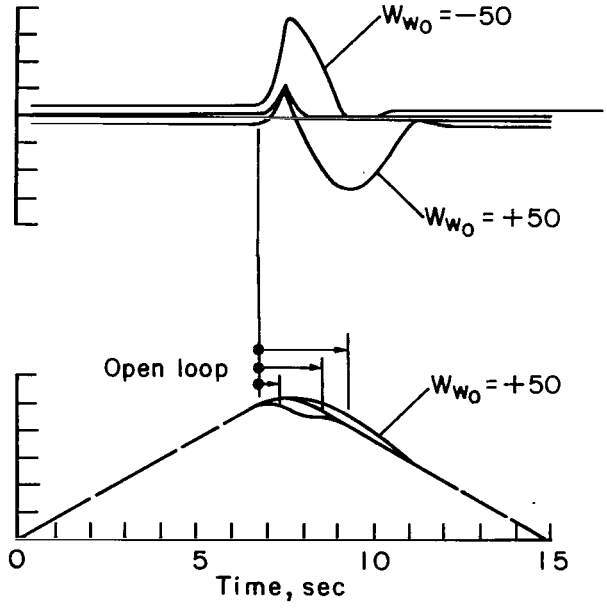


(e) Open-loop command (rate sensitive loop closing).

Figure 6.- Concluded.

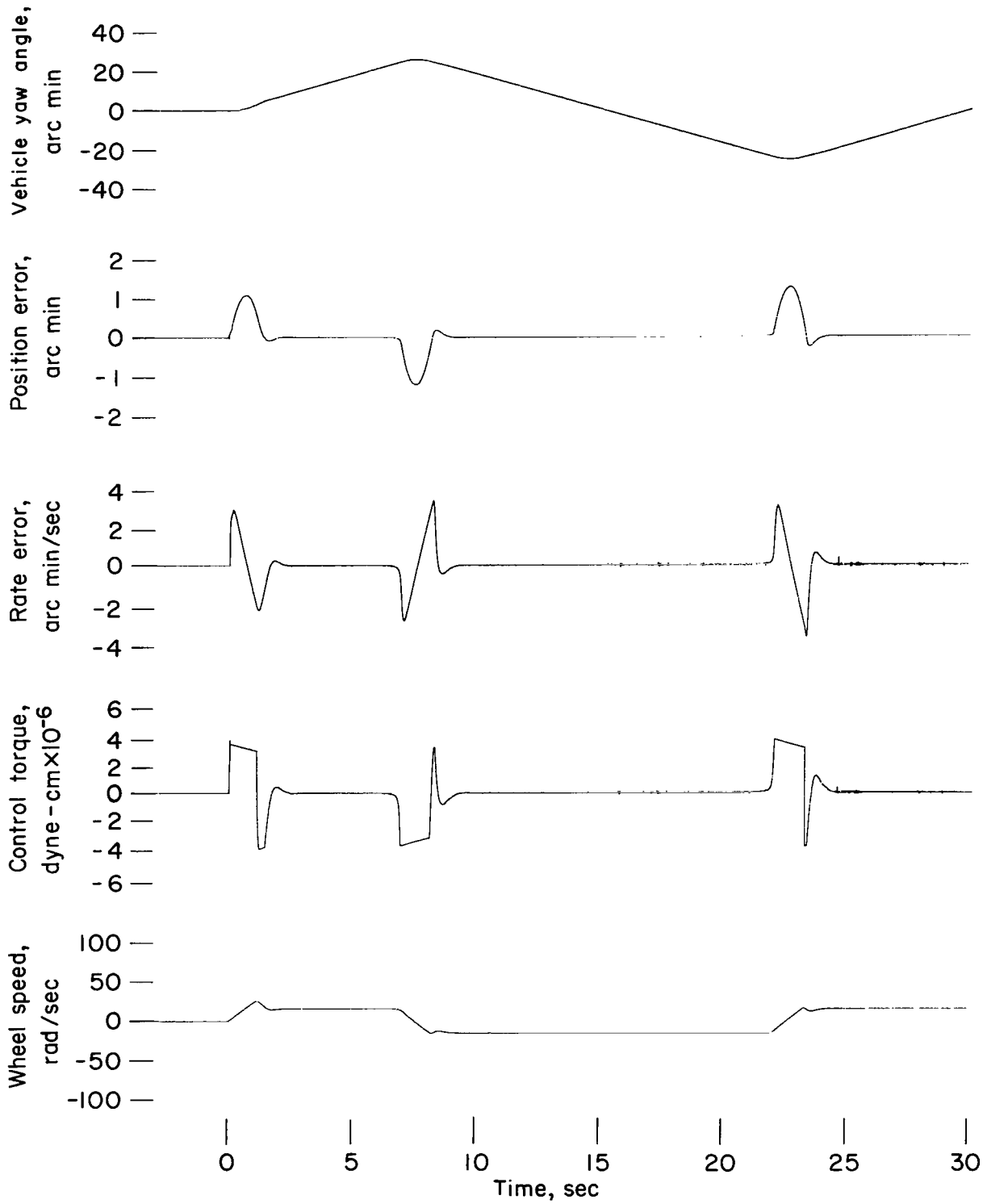


(a) Linear controller ($W_{w_o} = 0$).

Figure 7.- Dynamics of complete system performing scan and turnaround maneuver.

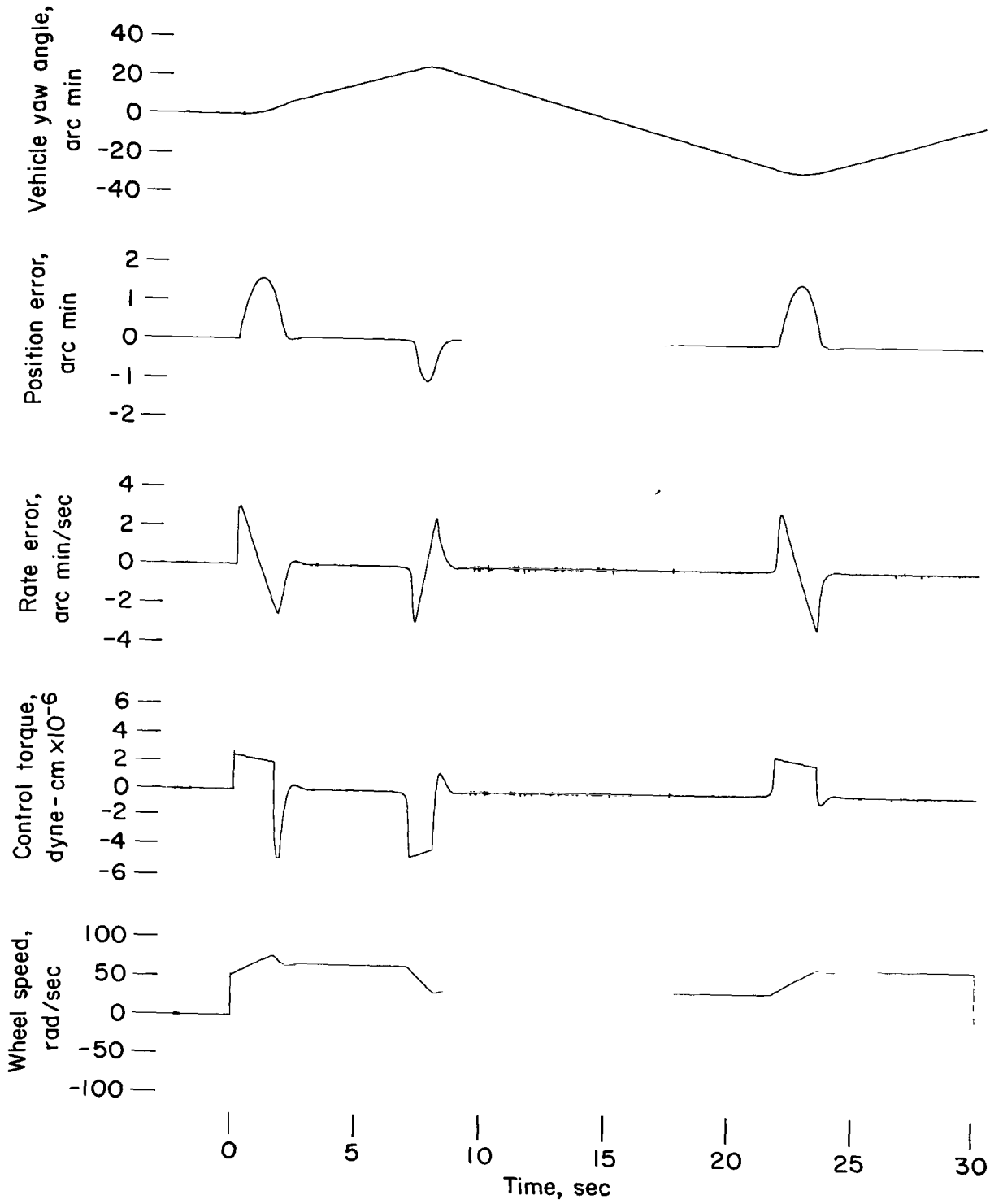


(b) Linear controller ($W_{w_o}$ = 50 rad/sec).

Figure 7.- Continued.

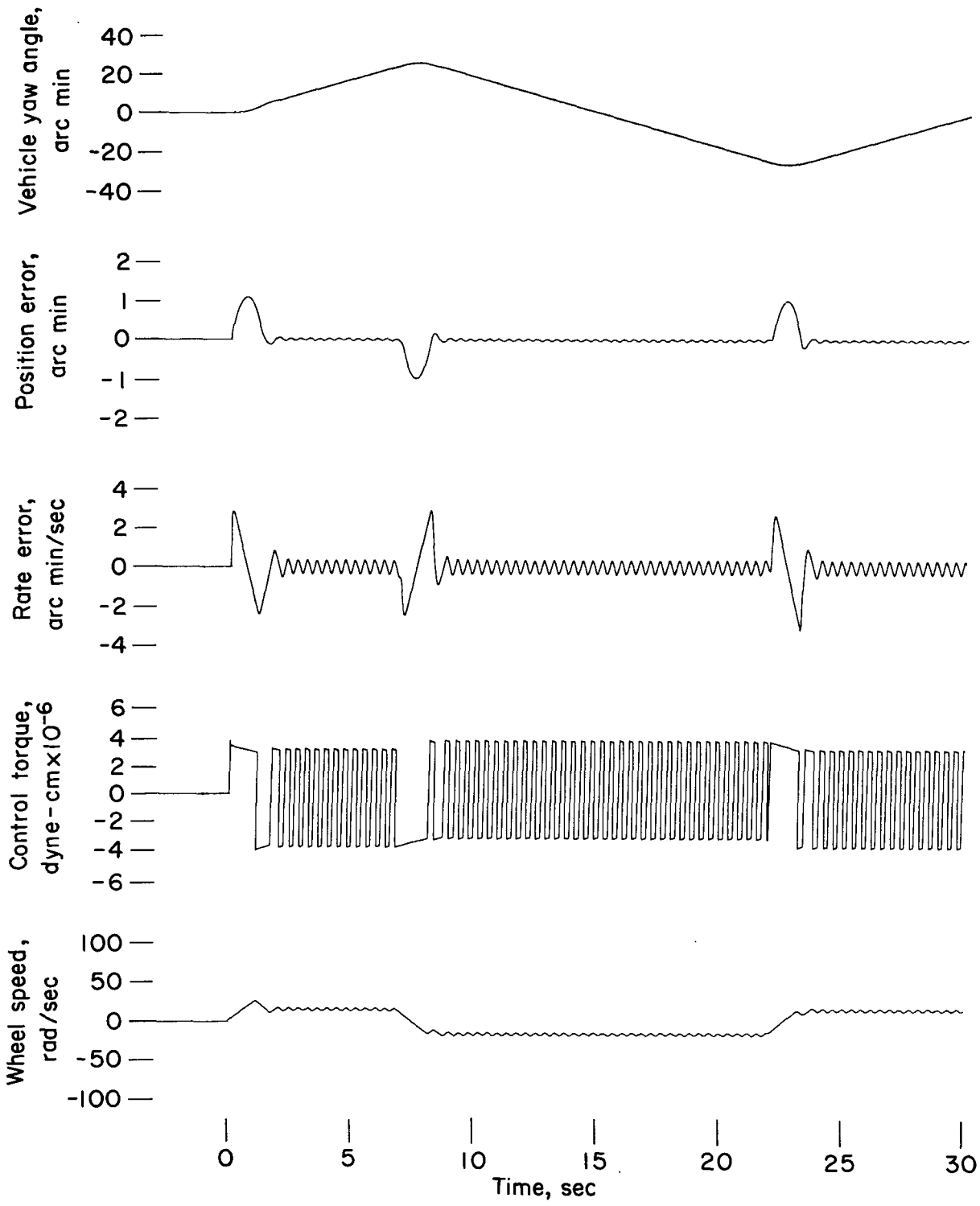


(c) Nonlinear controller ($W_{W_O} = 0$).

Figure 7.- Continued.

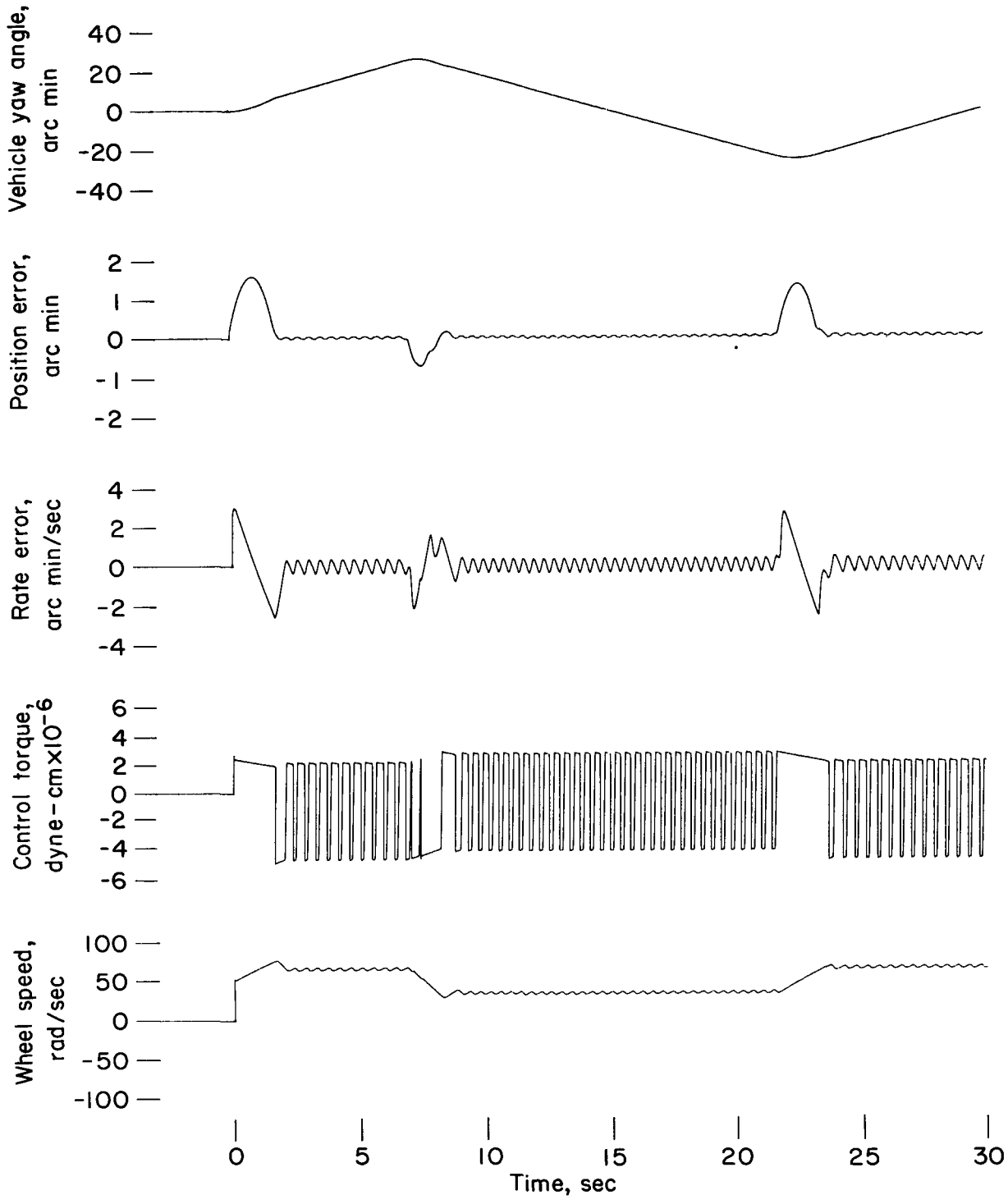


(d) Nonlinear controller ($W_{w_o}$ = 50 rad/sec).

Figure 7.- Continued.

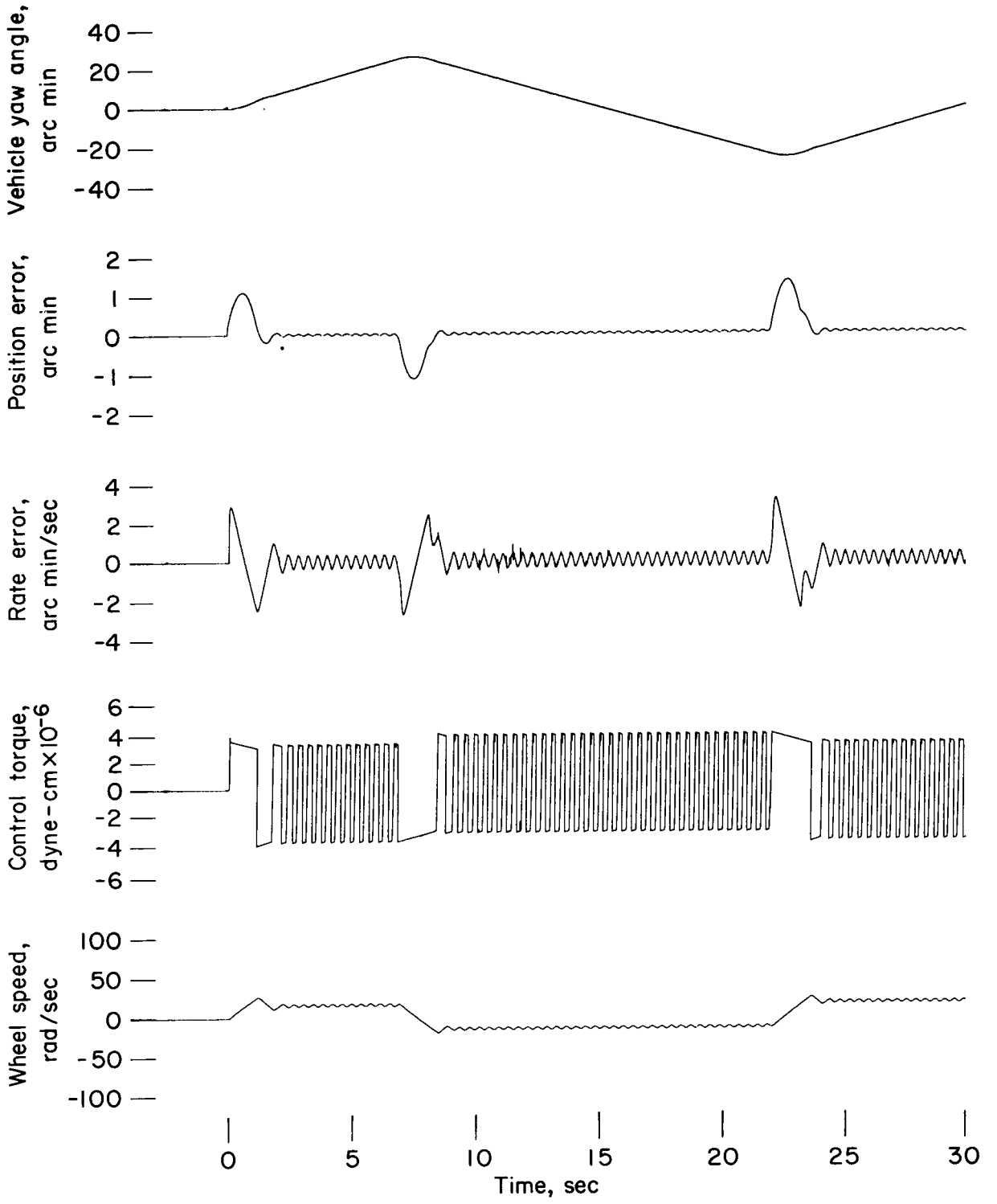


(e) Nonlinear controller, variable switching curve ($W_{W_O} = 0$).

Figure 7.- Continued.

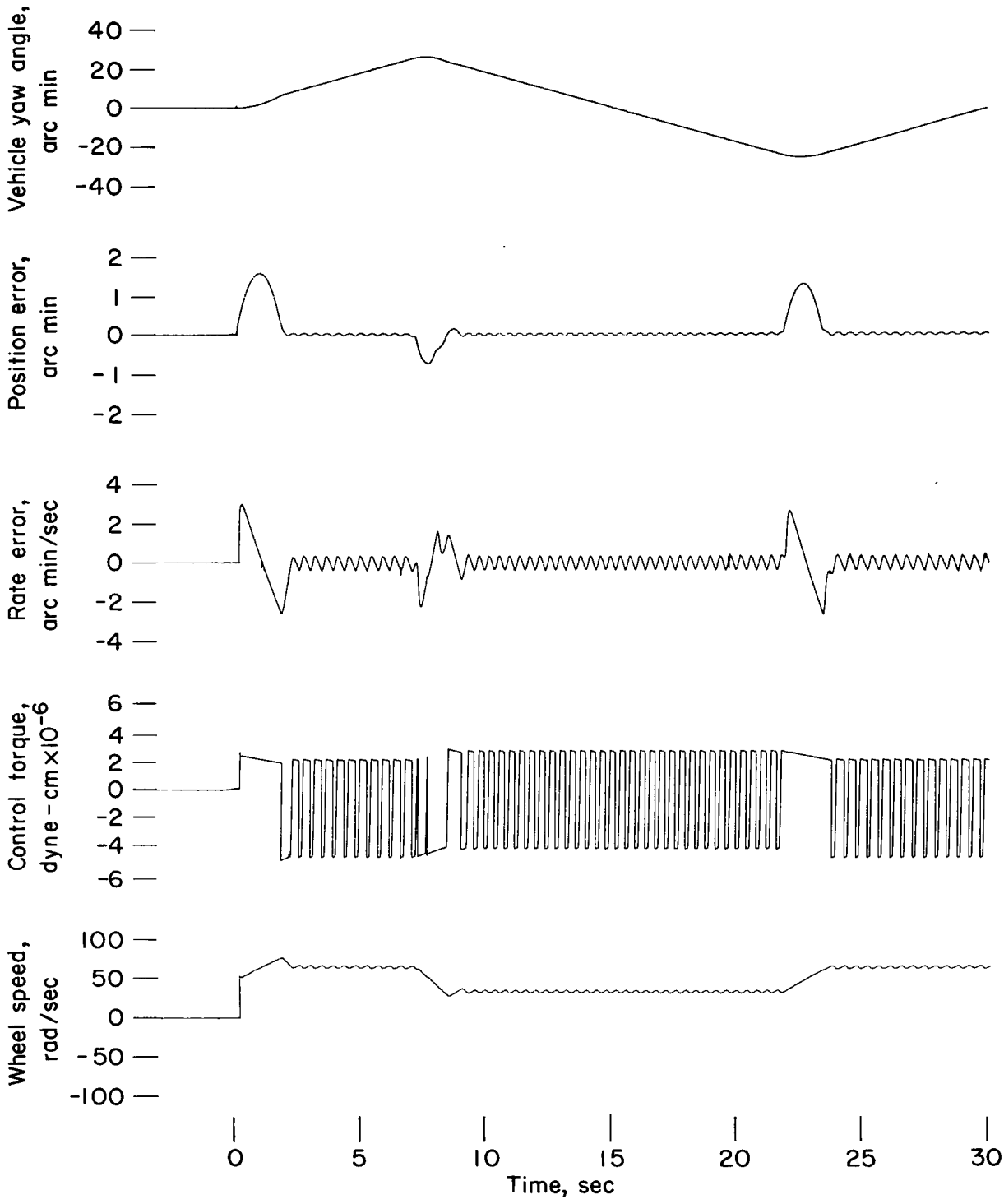


(f) Nonlinear controller, variable switching curve ($W_{wo}$ = 50 rad/sec).

Figure 7.- Continued.

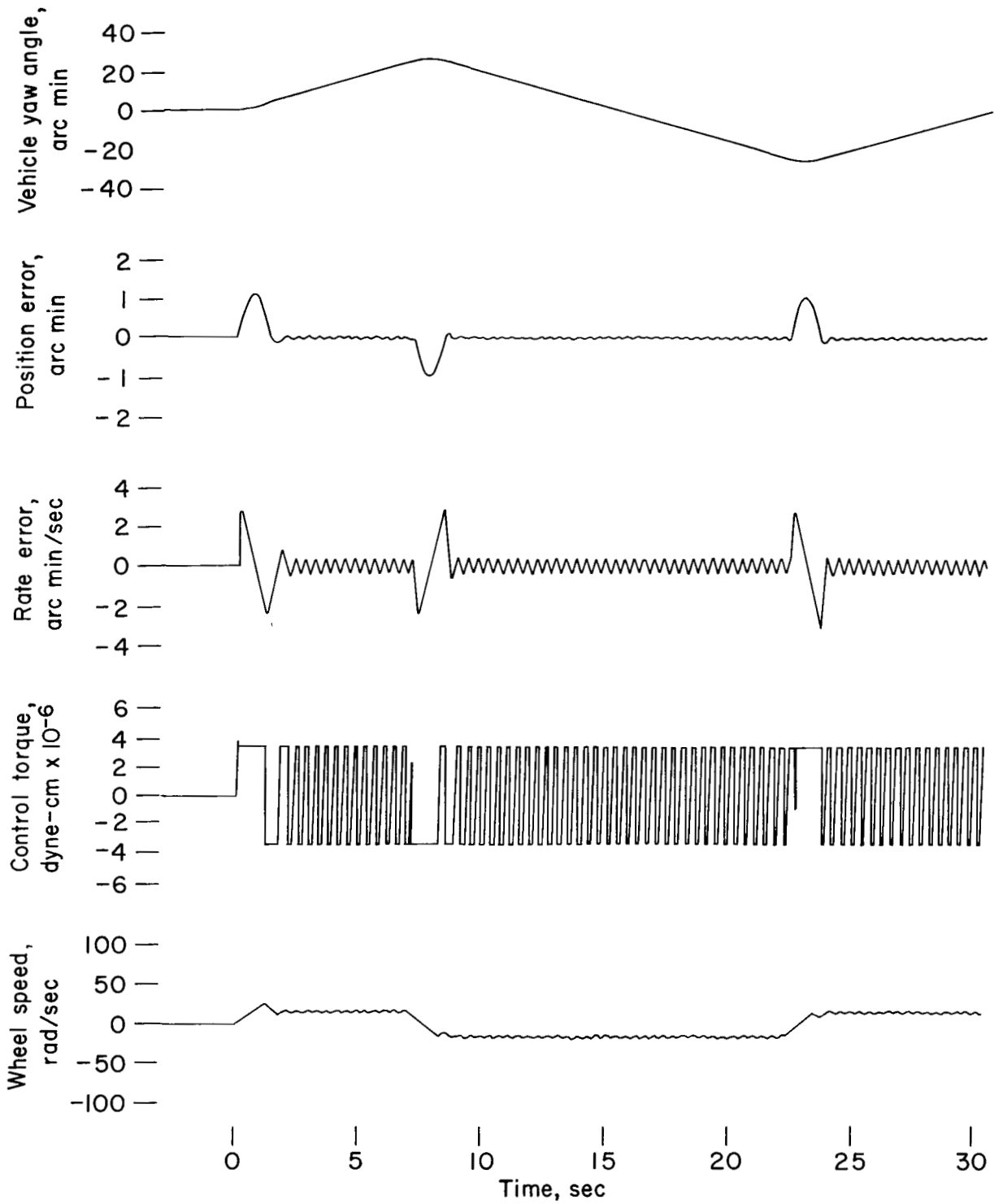


(g) Nonlinear controller ($\tau_m = \infty$), $W_{w_O} = 0$ rad/sec. (Performance is identical at $W_{w_O} = 50$ rad/sec.)

Figure 7.- Continued.

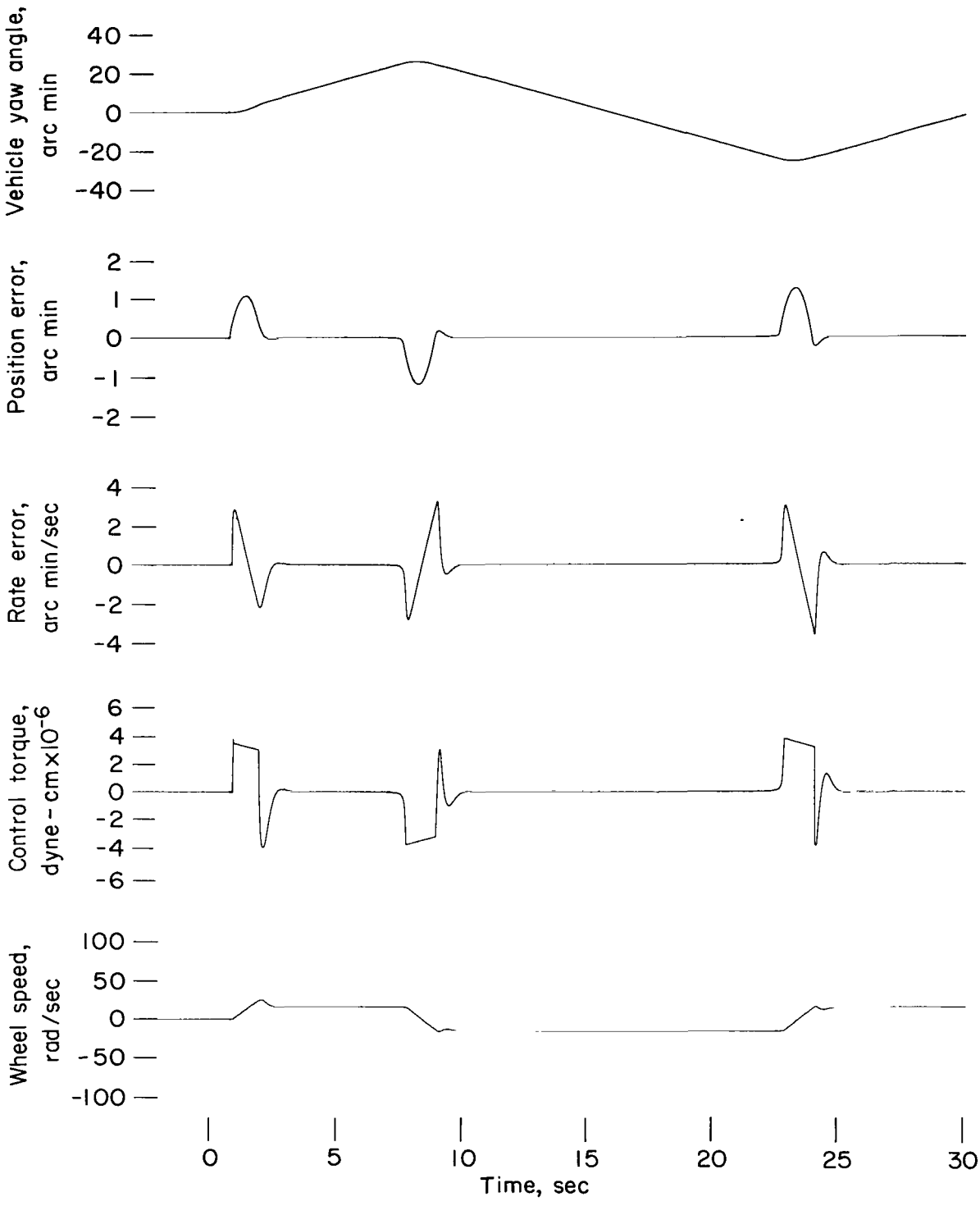


(h) Dual-mode controller ($W_{w_o} = 0$).

Figure 7.- Continued.

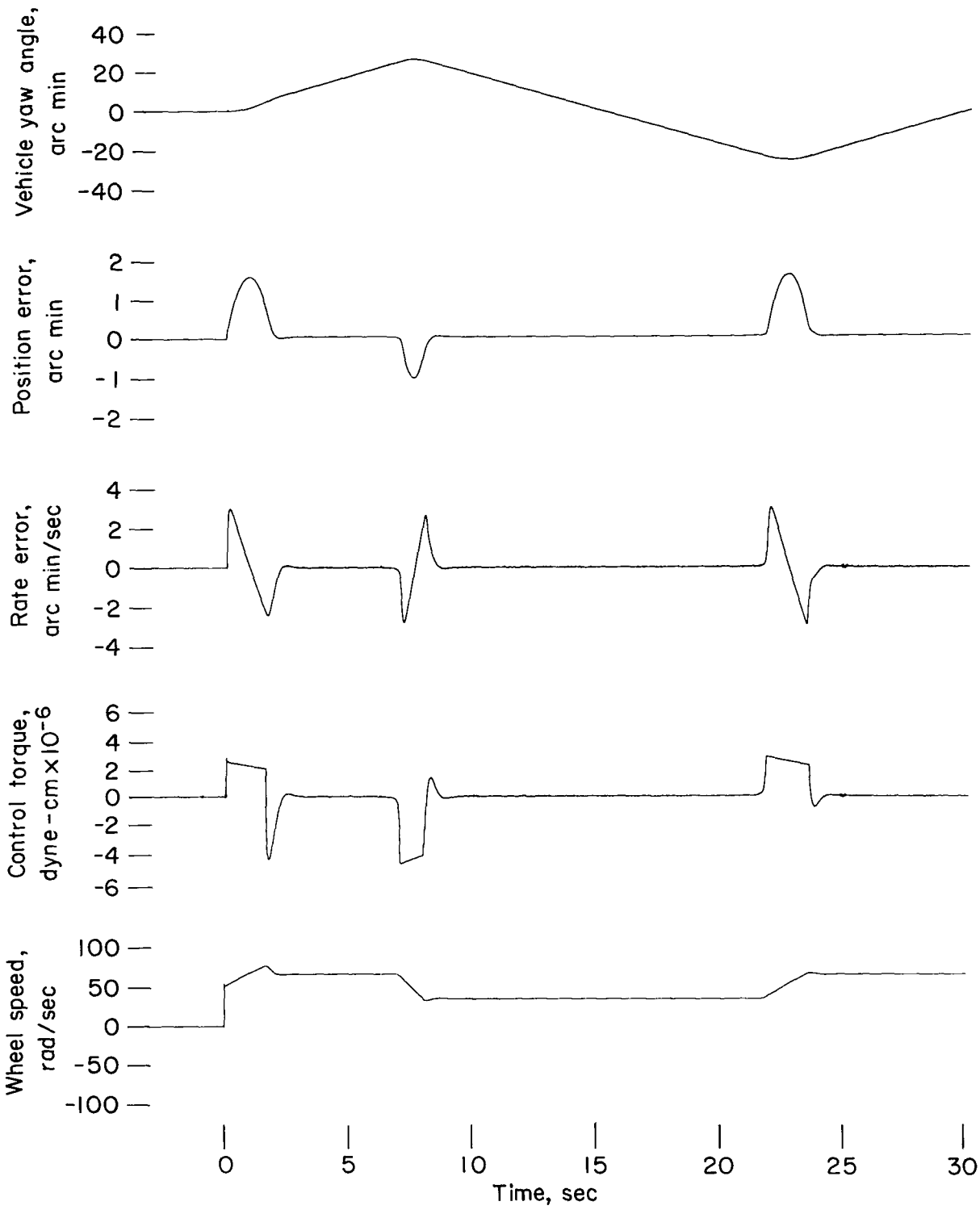


(i) Dual-mode controller ($W_{W_O}$ = 50 rad/sec).

Figure 7.- Concluded.

*"The aeronautical and space activities of the United States shall be conducted so as to contribute . . . to the expansion of human knowledge of phenomena in the atmosphere and space. The Administration shall provide for the widest practicable and appropriate dissemination of information concerning its activities and the results thereof."*

—NATIONAL AERONAUTICS AND SPACE ACT OF 1958

# NASA SCIENTIFIC AND TECHNICAL PUBLICATIONS

TECHNICAL REPORTS: Scientific and technical information considered important, complete, and a lasting contribution to existing knowledge.

TECHNICAL NOTES: Information less broad in scope but nevertheless of importance as a contribution to existing knowledge.

TECHNICAL MEMORANDUMS: Information receiving limited distribution because of preliminary data, security classification, or other reasons.

CONTRACTOR REPORTS: Technical information generated in connection with a NASA contract or grant and released under NASA auspices.

TECHNICAL TRANSLATIONS: Information published in a foreign language considered to merit NASA distribution in English.

TECHNICAL REPRINTS: Information derived from NASA activities and initially published in the form of journal articles.

SPECIAL PUBLICATIONS: Information derived from or of value to NASA activities but not necessarily reporting the results of individual NASA-programmed scientific efforts. Publications include conference proceedings, monographs, data compilations, handbooks, sourcebooks, and special bibliographies.

***Details on the availability of these publications may be obtained from:***

**SCIENTIFIC AND TECHNICAL INFORMATION DIVISION**

**NATIONAL AERONAUTICS AND SPACE ADMINISTRATION**

**Washington, D.C. 20546**